RIGA TECHNICAL UNIVERSITY
Faculty of Power and Electrical Engineering
Institute of Industrial Electronics and Electrical Engineering

Ugis SIRMELIS
Doctoral Student of the Study Programme "Computerised Control of Electrical Technologies"

URBAN ELECTRIC TRANSPORT SYSTEM MODELLING FOR THE SELECTION OF OPTIMAL ENERGY STORAGE PARAMETERS

Summary of the Doctoral Thesis

Scientific supervisors

Dr. sc. ing. L. LATKOVSKIS
Dr. sc. ing. J. ZAKIS

RTU Press

Riga 2015

DOCTORAL THESIS
PROPOSED TO RIGA TECHNICAL UNIVERSITY
FOR THE PROMOTION TO THE SCIENTIFIC DEGREE OF DOCTOR
OF ENGINEERING SCIENCES

To be granted the scientific degree of Doctor of Engineering Sciences (Dr. sc. ing.), the present Doctoral Thesis will be publicly presented on January 7, 2016 at the Faculty of Power and Electrical Engineering of Riga Technical University, Azenes Street 12/1, Room 212.

OFFICIAL REVIEWERS

Dr. habil. sc. ing. Ivars Rankis
Riga Technical University, Latvia

Dr. habil. sc. ing. Andris Sniders
Latvia University of Agriculture, Latvia

PhD Tonu Lehtla
Tallinn University of Technology, Estonia

DECLARATION OF ACADEMIC INTEGRITY

I hereby declare that the Doctoral Thesis submitted for the review to Riga Technical University for the promotion to the scientific degree of Doctor of Engineering Sciences (Dr. sc. ing.) is my own and does not contain any unacknowledged material from any source. I confirm that the Doctoral Thesis has not been submitted to any other university for the promotion to any other scientific degree.

Ugis Sirmelis …………………………….

Date: ………………………

The Doctoral Thesis has been written in Latvian. It consists of introduction, 4 chapters, conclusions, bibliography with 106 reference sources and 2 appendices. The volume of the present Doctoral Thesis is 110 pages. It has been illustrated by 91 figures and 10 tables.

Contents

General Description of the Doctoral Thesis

Topicality

Since the deposits of fossil fuels are running out, and at the same time the demand for energy is increasing, more and more attention is being paid to renewable energy sources, energy efficiency, and environmental protection. These cornerstones of sustainable energy policy are also put forward as essential issues within the European Union's economic development strategy, which determines that within the European Union by 2020 greenhouse gas emissions are to be cut down by 20 % (compared to 1990), the share of renewable energy is to be increased to 20 % and energy efficiency is to be increased by 20 % [1].

Although urban electric transport is regarded as a relatively clean type of transport in the urban environment, it should also be viewed as a potential direction, where it is possible to improve energy efficiency. For example, Ltd. Rigas Satiksme, which operates the public transport in Riga city, in recent years, on average has been consuming 60 GWh of electrical energy, which accounts for approximately 2.5 % out of all electrical energy consumption in Riga city [2]. Energy efficiency could be improved by more efficient use of regenerated braking energy of trams and trolleybuses. Currently regenerated energy is being partly dissipated in brake resistors, and approximately 2 GWh of electrical energy is wasted this way in Riga every year [3]. Fitting electric transport system with reversible traction substations or energy storage systems allows reducing the amount of braking energy that is dissipated in brake resistors. Introduction of regenerative braking energy saving technologies is expensive; therefore, it is very important to optimise parameters of these systems in order to maximise their performance.

Goal and Objectives of the Research

The main goal of the research is to study what supercapacitor (SC) energy storage system (ESS) parameter values should be chosen in order to maximise the performance of such systems. To achieve the goal, the following objectives have been set:

- to develop the mathematical model, which allows the simulation of public electric transport system that contains SCs based ESS;
- to develop the method, which determines the optimal power and energy capacity parameters for mobile and stationary energy storage systems;
- to investigate the influence of energy storage system control parameters on recoverable energy amount.

Research Methods and Tools

- *Matlab* has been used to develop simplified mathematical models of public electric transport system and process experimentally measured tram power diagrams.
- *Matlab/Simulink* has been used to develop a simulation model of public electric transport system, analytic simulation model of energy storage system and its control circuits.
- *PSim* has been used to demonstrate the method, which allows the simplification of equivalent electrical circuit of contact lines.
- A program that calculates trolleybus contact line resistances has been developed in *MS Excel*.
- Tram power diagrams have been obtained on trams T3A.
- For demonstration of the proposed voltage measuring system, the equipment of the Institute of Physical Energetics has been used.

Scientific Novelties

- A new method that allows the determination of number of SCs in an energy storage system. The proposed method allows the estimation of profitability of variously sized energy storage systems.
- Use of isolated DC/DC converter to set the reference voltage for comparators in order to measure individual cell voltages for series connected SCs.
- A detailed *Matlab/Simulink* simulation model for a tram system with radial feeding topology.
- Analytic current and voltage equations of series connected RLC circuit are used to describe the operation of energy storage system, which is made of buck & boost converter and SC battery. Fast and accurate simulation model of energy storage system in *Matlab/Simulink* has been developed based on these equations.

Practical Significance of the Research

- The proposed energy storage system sizing method can be used to estimate whether it is rational to equip specific substations with energy storage systems.
- *Matlab/Simulink* model of electric transport system can be used as a tool to assess the existing infrastructure capacity reserve and to determine weak points in the contact line. It can be useful in planning tram cruising intensity or assessing the use of public electric transport infrastructure to charge electric vehicles.
- The proposed voltage measurement system can be used not only for SCs, but also for other energy storage technologies.

Dissemination of Results

The main results of this thesis have been presented in the following international scientific conferences:

- 14th European Conference on Power Electronics and Applications "EPE 2011 ECCE Europe", Birmingham, UK, 30 August – 1 September 2011.
- 9th International Conference on Compatibility and Power Electronics "CPE 2015", Caparica, Portugal, 24–26 June 2015.
- 9th International Conference on Electrical and Control Technologies "ECT 2014", Kaunas, Lithuania, 8–9 May 2014.
- 5th International Conference on Power Engineering, Energy and Electrical Drives "Powereng 2015", Riga, Latvia, 11–13 May 2015.
- 12th International Scientific Conference "Engineering for Rural Development", Jelgava, Latvia, 23–24 May 2015.
- 14th International Scientific Conference "Engineering for Rural Development", Jelgava, Latvia, 20–22 May 2015.
- 5th European Symposium on Super Capacitors & Hybrid Solutions "ESSCAP 15", Brasov, Romania, 23–25 April 2015.

Publications

- L. Latkovskis, U. Sirmelis, and L. Grigans, "On-board Supercapacitor Energy Storage: Sizing Considerations", Latvian Journal of Physics and Technical Sciences, vol. 49, no. 2, pp. 24–33, 2012.
- U. Sirmelis, "Braking Energy Recovery in Tram Systems Using Supercapacitors", in Proceedings of the 9th International Conference on Electrical and Control Technologies, Kaunas, Lithuania, 2014, pp. 138–141.

- U. Sirmelis, J. Zakis, and L. Grigans, "Optimal Supercapacitor Energy Storage System Sizing for Traction Substations", in Proceedings of the conference POWERENG 15, Riga, Latvia, 2015, pp. 592–595.
- U. Sirmelis, L. Grigans, and L. Latkovskis, "An Analytic Simulation Model for a Supercapacitor-based Energy Storage System", in Proceedings of the 14th European Conference on Power Electronics and Applications, Birmingham, UK, 2011, pp. 1–10.
- U. Sirmelis, "ESS Sizing Considerations According to Control Strategy", in Proceedings of the conference "Engineering for Rural Development", Jelgava, Latvia, 2013, pp. 346–351.
- U. Sirmelis, L. Grigans, J. Zakis, "Isolated DC/DC Converter Based Voltage Measuring System for Series Connected Supercapacitor Cells", in Proceedings of CPE2015 conference, Caparica, Portugal, 2015, pp. 443–446.
- U. Sirmelis, L. Grigans "Stationary ESS Control According to Tram Traffic Intensity", in Proceedings of the conference "Engineering for Rural Development", Jelgava, Latvia, 2015, pp. 377–382.
- L. Grigans, U. Sirmelis, K. Kroics, "Optimal Supercapacitive Energy Storage Sizing for Mobile Application", in Proceedings of the 5th European Symposium on Super Capacitors & Hybrid Solutions, Brasov, Romania, 2015, pp. 11-17.

Introduction

The use of SCs in ESSs, which recover braking energy, is topical since 1990, when SCs with good power properties became available [4]. Research on SC usage in public electric transport systems was initiated in 2000, when *Siemens* started to develop stationary ESS *Sitras SES*. In 2003, the first Sitras SES devices were tested in Madrid, Cologne and Dresden [5].

One of the first who studied SC application in public electric transport systems was a group of scientists from Switzerland. Over the period 2003–2007, they studied both stationary and mobile use of ESS. In their research they concluded that fitting trams with SCs based ESS allowed reducing electrical energy consumption by 25.6 % [6]; however, the choice of ESS energy capacity and power parameters was not justified. This means that the savings made by ESS in the long term may not be sufficient to cover the cost of ESS installation. In the research on a stationary ESS, they analyse the opportunity to use ESS as an alternative to building a new traction substation in order to reduce voltage drop in overhead contact lines [7].

Research on this topic has also been carried out in Belgium. In the research on mobile ESS application in metro and tram systems, various ESS control strategies are studied. The attention is also paid to ESS sizing. It is concluded that the ESS which contains the highest number of SCs gives the best results; however, the issue of profitability of such a system is put forward for discussion [8], [9], [10]. An algorithm that controls charge and discharge process is proposed for stationary ESS. Energy consumption of tram system is analysed for scenarios where multiple, variously sized ESSs are placed at different tram route locations. The obtained results show that the overall energy consumption in a tram system can be reduced by 11 to 26 % [11], [12].

Research on SCs based ESS application in metro systems has been carried out at the University of Naples Federico II. Several studies deal with the problem of optimal choice of SCs in SC battery. The optimisation of SC battery is carried out in order to reduce the maximum current from a substation and to reduce voltage fluctuations at metro train input [13], [14]. Control algorithm of mobile ESS is proposed and profitability of ESS is analysed in [15]. Various control algorithms for stationary ESSs are proposed and compared. Multiobjective optimisation is carried out in order to optimise energy savings and stabilize overhead contact line voltage [16]–[20].

Research on this topic has also been carried out at Tallinn University of Technology (TTU), and Institute of Physical Energetics (IPE). At TTU, various technologies that allow reducing energy consumption in tram systems are analysed. Stationary and mobile SCs based ESSs are studied; however, more attention has been paid to mobile ESSs. Economic calculations have been made to assess the return on investment for specific ESS [21], [22]. A method that allows estimating energy amount wasted in brake resistors and variously sized ESS effect on tram system energy consumption can be highlighted as the main research results of IPE in this field [23], [24].

In the present research, various parameters for SCs based ESS are studied and economic considerations are carried out in order to improve performance of such systems. Optimisation for power and energy capacity parameters of ESS is made and optimum values for ESS control parameters are determined.

1. Technologies for Braking Energy Recovery in Urban Rail Transport Systems

1.1. Commercialised Energy Storage Systems

Currently several companies offer products that allow recovering braking energy; however, their application in real systems is still very rare. Table 1 shows the list of commercialised stationary energy storage systems that are based on various technologies.

Table 1

Commercialised Braking Energy Recovery Systems

Technology	Company	Brand name	Application in real systems	References
Flywheels	*Piller Power Systems*	*Powebridge*	Hannover, Hamburg, Rennes	[25], [26]
	Calnetix	*Vycon® Regen®*	Los Angeles	[27]
Li-ion batteries	*SAFT*	*Intensum Max*	Philadelphia	[28]
	Toshiba	*TESS*	Tokyo	[29]
	Hitachi	*B-Chop*	Kobe, Macau, Hong Kong	[25], [30]
Ni-MH batteries	*Kawasaki*	*BPS*	Osaka, Tokyo Hokkaido	[25], [31]
Supercapacitors	*Siemens*	*Sitras SES*	Madrid, Cologne, Beijing, Nuremberg, Rotterdam, Toronto, Portland	[32], [33]
	ABB	*Enviline*	Philadelphia, Warsaw	[25], [34]
	Adetel	*NeoGreen Power*	Lyon	[25]
	Woojin		Seoul	[35], [36]
	Meidensha Cooperation	*CapaPost*	Japan	[25], [37]
Reversible substations	*Siemens*	*Sitras TCI*	Oslo, Singapore	[25], [38]
	ABB	*Enviline ERS*	Lodz	[25]
	Alstom	*HESOP*	Paris, London, Milan	[39]
	Ingeteam	*Ingeber*	Bilbao, Malaga, Brussels, Bielefeld	[40]–[43]

1.2. Supercapacitor Voltage Measuring System

As can be seen in Fig. 1.1, the proposed voltage measuring system is based on a single-ended isolated forward converter, which has many transformers with common primary winding and equal number of turns in secondary windings. The particular converter topology is chosen due to its simple control; however, other topologies can also be considered.

Control and measurement unit (CMU) sets reference voltage (v_{ref}) and controls duty cycle *D* for transistors VT1 and VT2 to match filter capacitor voltages ($v_{C1} - v_{Cn}$) to reference voltage. Each filter capacitor voltage is compared to SC cell voltage with the use of comparators (CMP1 — CMP*n*). If the voltage across any filter capacitor is higher than the voltage of matching SC cell (SC1 — SCn), the corresponding comparator sets its output to 1, which means that particular SC cell voltage is lower than the reference voltage. Comparator output signal is filtered, to prevent oscillations, and then sent to CMU via isolated communication, which is not considered in the present research.
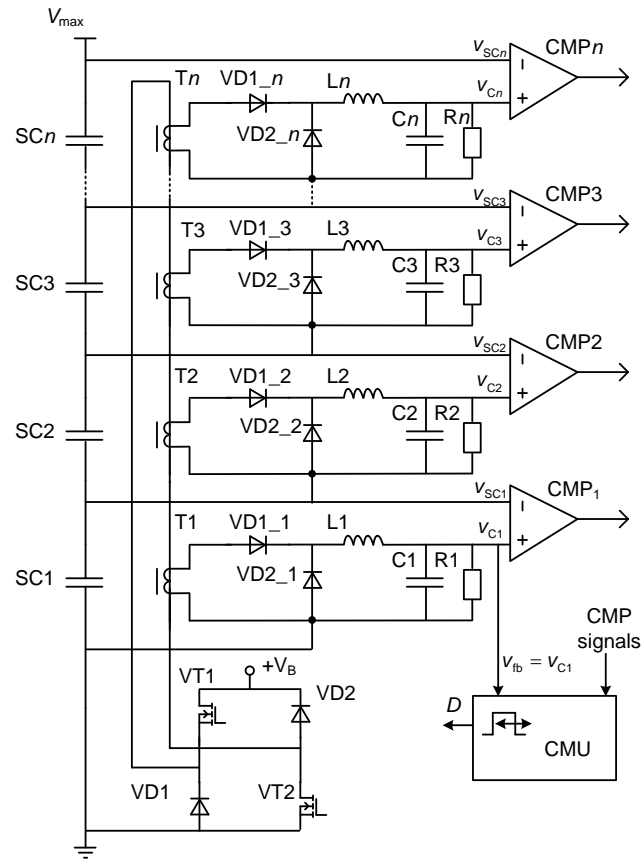
Fig. 1.1. The proposed voltage measuring system for series connected SCs.

To verify the functionality of proposed voltage measuring system, its prototype was made, and it is partly shown in Fig. 1.2.
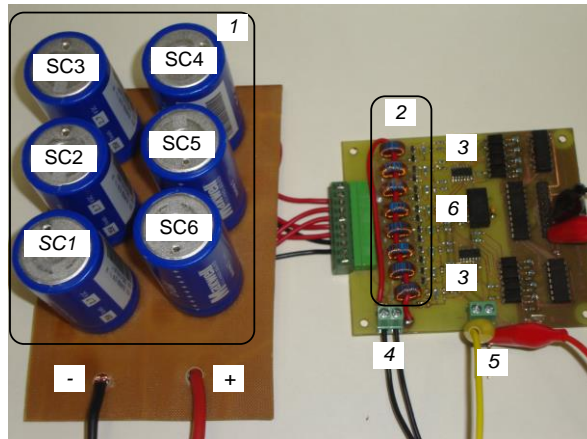

Fig. 1.2. The proposed voltage measuring system for series connected SCs (1. SC battery; 2. transformers and filters; 3. comparators; 4. input voltage for primary side; power supply for DC/DC converters; 6. +/− 15 V isolated DC/DC converter, which powers comparators).

Fig. 1.3 depicts the results of a test where system prototype was operated in Max/min mode and 4 signals were measured: CMP6 — comparator, which monitors SC with the highest potential, v_{C1} — reference voltage measured on a filter capacitor with the lowest potential, v_{sc6} and v_{sc1} — voltages of SCs with the highest and lowest potential, respectively. SCs had various initial voltages and were charged with 25 A current. When SC6 voltage reaches 2.5 V value, which matches the reference voltage, corresponding comparator CMP6 changes its output state from high to low, which demonstrates correct functionality of the proposed measuring system.
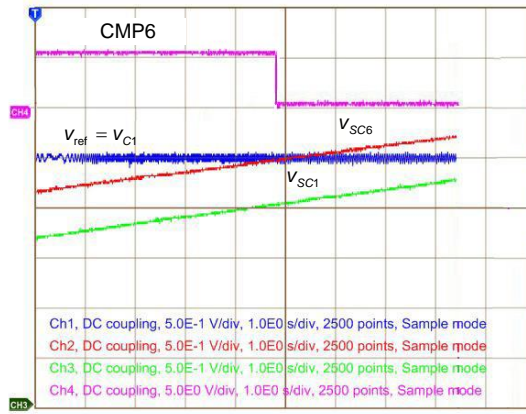
Fig. 1.3. Operation of the proposed system in Max/min mode.

2. Simulation of Public Electric Transport System Equipped with Mobile Energy Storage System

Fig. 2.1 shows a radial topology feeding infrastructure of public electric transport system. The feeding area of one substation is divided into several sections, which typically are less than a kilometre long. Each section starts and ends with a non-conducting fragment in overhead feeding line (section isolators). Each section is connected to a traction substation with one or more feeding cables. To reduce the voltage sags in overhead contact lines, potential equalizers are used. Potential equalizers connect the overhead contact lines in places where traffic is organised in both directions; thus, total line resistance is reduced.
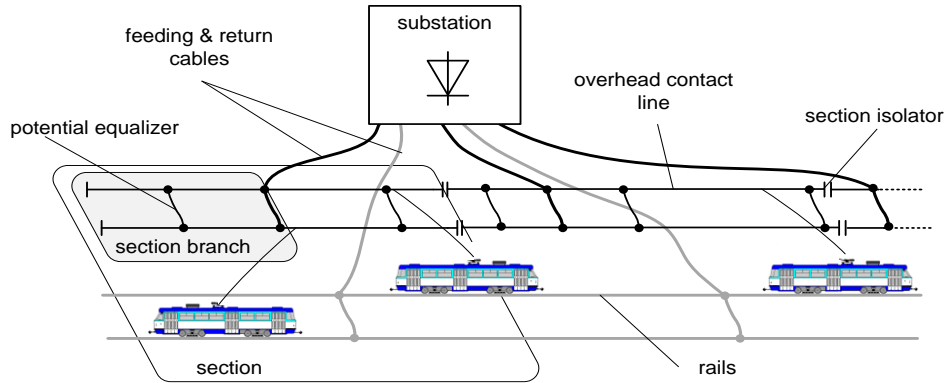

Fig. 2.1. Public electric transport system with a radial feeding topology.

2.1. Method for Obtaining the Simplified Equivalent Electrical Circuit of Overhead Contact Line

The resistance of overhead contact line between a moving tram and a feeding cable connection point has a variable value. The lowest value is at feeding cable connection point, but the highest — at the end of the feeding section.

It is convenient to obtain the simplified equivalent circuit of overhead contact line by using some electric circuit simulation software. The method proposed in the present research will be demonstrated using *PSim*. This method contains 5 stages.

1. An equivalent circuit is made as shown in Fig. 2.2. Overhead contact lines of each section branch are substituted by equivalent resistances R_{L1} — R_{L5}, while resistors R_{sl1} — R_{sl5} are substitute for rails matching the length of the corresponding section branch. Equivalent resistances of feeding and return cables are modelled by resistors R_{k1} — R_{k5}.
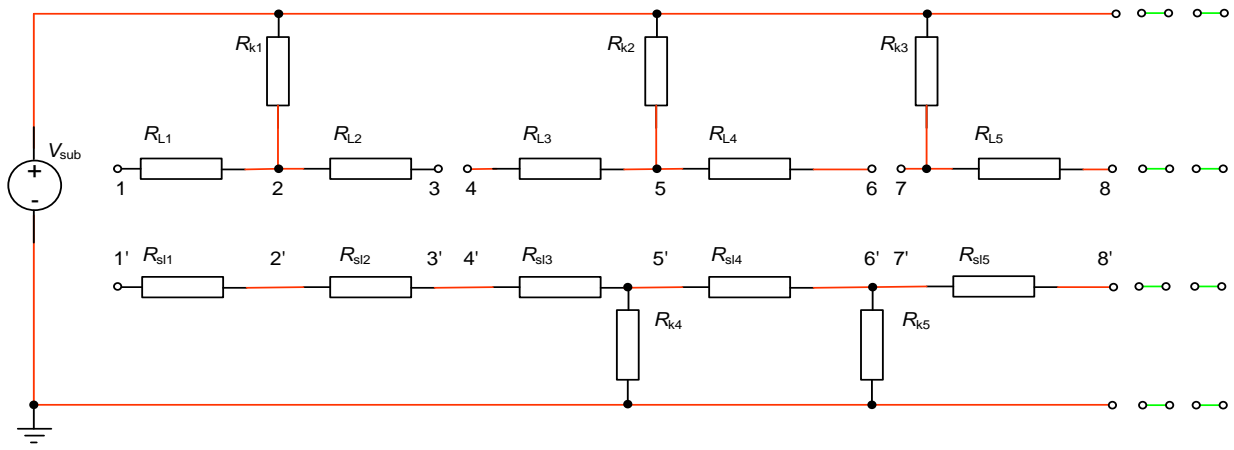
Fig. 2.2. Equivalent circuit of tram feeding infrastructure.

2. Values of resistors in Fig. 2.2 are calculated. Rk1 – Rk5 are calculated by multiplying the length of the cable with its dc resistance (Ω/km). Resistances of rails and overhead contact lines are calculated in a similar manner; besides, it is assumed that potential equalizers are placed at both ends of each section branch.

3. Resistances between nodes 1–1', 2–2', etc. are determined. A convenient way of doing this is by replacing voltage source V_{sub} with current source and connecting voltmeter in "+" wire. By making the short circuit between nodes 1–1', 2–2', etc. and setting current source to value of 1000 A the equivalent resistance between these nodes expressed in mΩ can be read directly from a voltmeter.
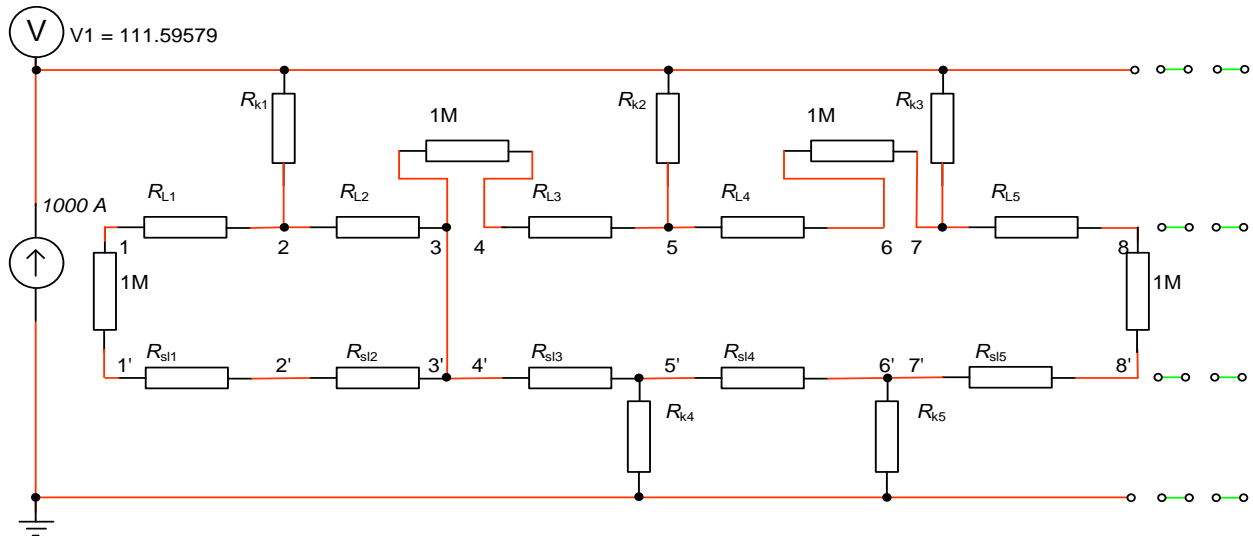

Fig. 2.3. *PSim* model for determination of resistance between nodes 1–1', 2–2', etc.

4. Simplified model is made with all the resistances in the "+" wire as it is shown in Fig. 3.
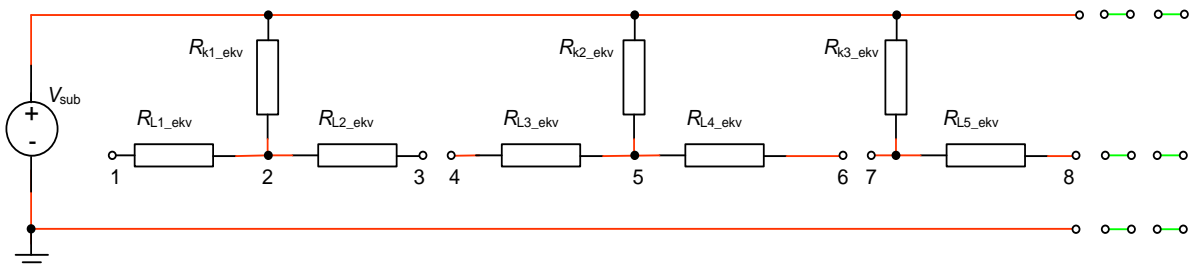

Fig. 2.4. Simplified model of tram feeding infrastructure with all resistances in "+" wire.

5. Values of simplified circuit resistors are calculated as shown in Table 2.

Table 2

Calculation of Equivalent Resistances

Resistance	R_{k1_ekv}	R_{k2ekv}	R_{k3ekv}	R_{L1_ekv}	..	R_{L5_ekv}
Value	R(2–2′)	R(5–5′)	R(8–8′)	R(1–1′) – R(2–2′)	..	R(8–8′) –R(7–7′)

2.2. Simulation of Tram System in *Matlab/Simulink*

Variable Resistance Model

Simulation of overhead contact lines requires the model of resistors, which can change a resistance value during simulation. Since there is no such model in *Matlab/Simulink*, a variable resistor is made as a resistor matrix (see Fig. 2.5).
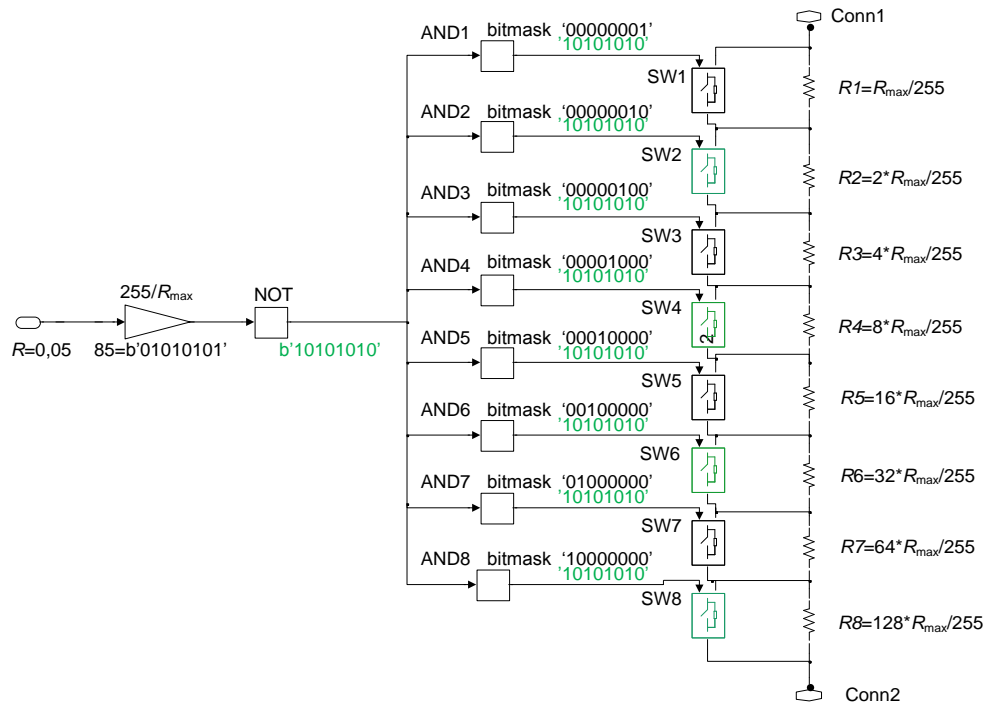
Fig. 2.5. Model of variable resistor in *Matlab/Simulink*.

Substation Model

In order to ensure fast simulation of traction substation, its simplified model is made as shown in Fig. 2.6. Such a model allows obtaining I–V curve, which is typical for traction substations with a six-phase rectifier with an interphase transformer.
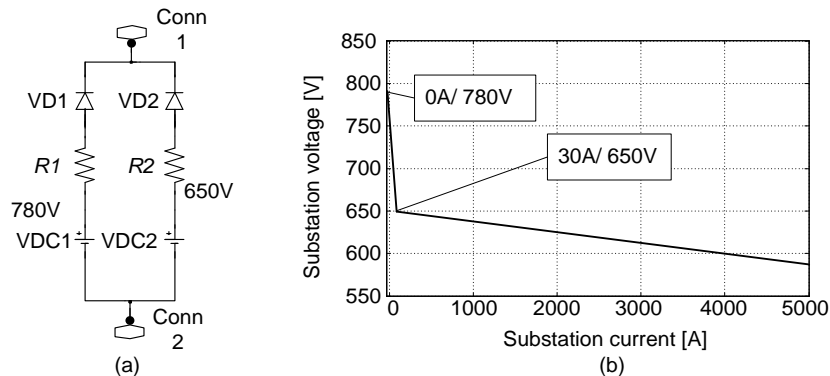

Fig. 2.6. Simulink model of traction substation and its I–V curve.

Tram Model

The simulation model of a tram is based on controlled current source CCS as it is shown in Fig. 2.7. CCS value is calculated by dividing tram power Pin by the voltage measured over current source. Positive P_{in} values correspond to the running mode of tram, while negative values — to the braking mode. Blocks S1 and min are introduced to limit tram current in cases when tram input voltage reaches 400 V. By the use of 780 V voltage source VDC and diode VD1 the functionality of braking chopper is ensured.
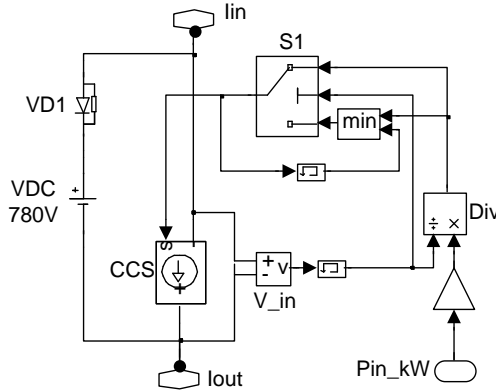

Fig. 2.7. Tram model in *Simulink*.

Model Verification

The operation of the model is demonstrated with a partial model of Riga 10th traction substation feeding area, which is shown in Fig. 2.8. Blocks R1$_{se1}$, R2$_{se1}$, R3$_{se1}$ and R4$_{se1}$ contain models of variable resistors, but blocks P1$_{se1}$, P2$_{se1}$, P3$_{se1}$ and P4$_{se1}$ contain tram models.
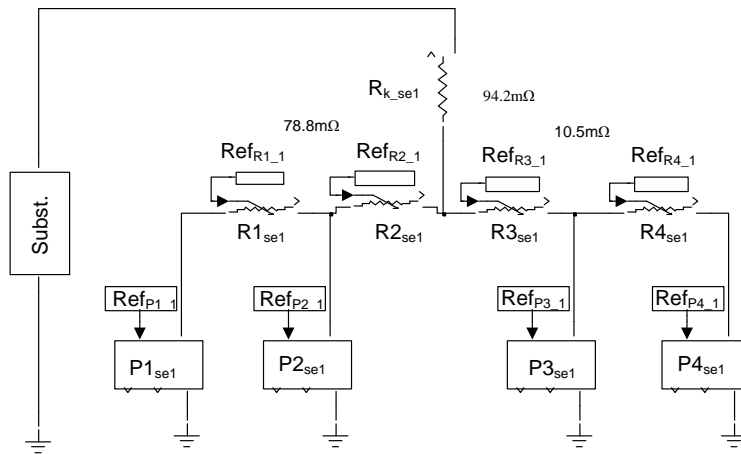

Fig. 2.8. *Simulink* model of 1 section of Riga 10th traction substation.

Tram system model operation diagrams of scenario where 2 trams moving in opposite directions are crossing this feeding section are shown in Fig. 2.9.
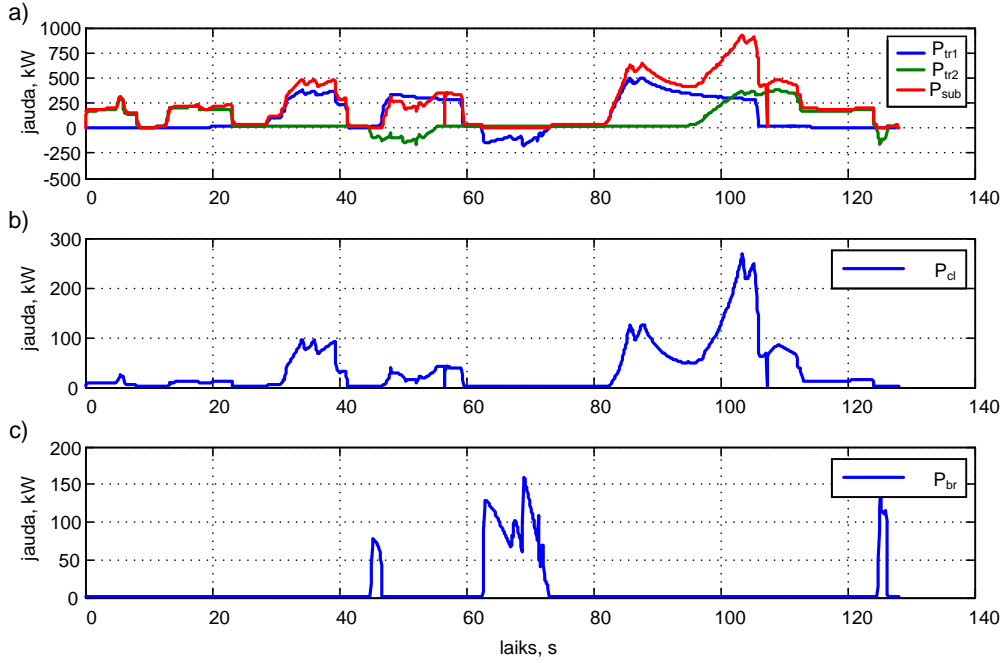
Fig. 2.9. Operation diagrams of tram system model; a) power diagrams of trams and substation; b) losses in overhead contact lines and feeding cable; c) power dissipated in braking resistors.

2.3. Analytic Model of Energy Storage System

To describe the operation of SCs based ESS power stage (see Fig. 2.10) with analytic equations, two assumptions are made:

- IGBT transistors VT1, VT2 and diodes VD1, VD2 are considered to be ideal switches with no active losses;
- high capacity capacitor is at the input of ESS, which acts similarly to voltage source.

Taking into account these assumptions, ESS power stage can be viewed as series connected RLC circuit, which periodically is connected to voltage source or short circuited. In this case, R_{eq} is substitute for SC battery internal series resistance and inductor resistance, L is inductance of DC/DC converter inductor, but C_{SC_b} is capacitance of SC battery.
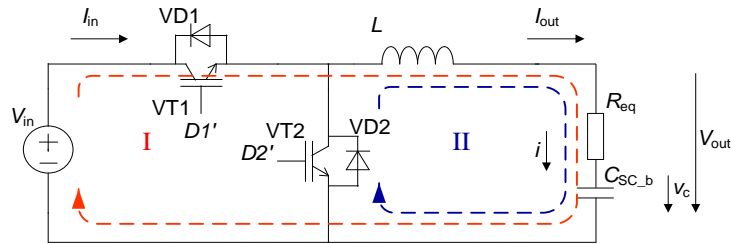

Fig. 2.10. Power stage of ESS, which contains buck & boost converter and SC battery.

In the time interval $0 < t < D1' \cdot T$ (when the IGBT VT1 is switched on), the converter is operating in the buck mode, and the energy is transferred from the external voltage source V_{in} to SC battery. While VT1 is conducting, R_{eq}, L and C_{SC_b} are connected to V_{in} thus closing the current loop I. Current i and SC voltage v_C in this state can be calculated as:

$$i(t) = e^{-bt}\left((V_{in} - V_C(0))\frac{1}{\omega_0 L}\sin\omega_0 t + I(0)\left(\cos\omega_0 t - \frac{b}{\omega_0}\sin\omega_0 t\right)\right), \tag{2.1}$$

$$v_C(t) = V_{in} - e^{-bt}\left((V_{in} - V_C(0))\left(\cos\omega_0 t + \frac{b}{\omega_0}\sin\omega_0 t\right) - \frac{1}{\omega_0 C_{SC\_b}}I(0)\sin\omega_0 t\right), \tag{2.2}$$

15

where:

$$b = \frac{R_{eq}}{2L}, \quad \omega_0 = \sqrt{\frac{1}{LC_{SC\_b}} - \frac{R_{eq}^2}{4L^2}},$$

0<t<D1'T — time counted from beginning of period, s;

I(0)   — current at the beginning of period, A;

$V_C(0)$ — voltage across C_{SC_b} at the beginning of period, V;

D1' — IGBT VT1 duty cycle.

When VT1 is switched off, the freewheeling diode VD2 starts to conduct and the current closes through loop II. The values of *i* and v_C can be calculated as:

$$i(t_2) = e^{-bt_2}\left(-V_C(D1'T)\frac{1}{\omega_0 L}\sin\omega_0 t_2 + I(D1'T)\left(\cos\omega_0 t_2 - \frac{b}{\omega_0}\sin\omega_0 t_2\right)\right), \quad (2.3)$$

$$v_C(t_2) = -e^{-bt_2}\left(-V_C(D1'T)\left(\cos\omega_0 t_2 + \frac{b}{\omega_0}\sin\omega_0 t_2\right) - \frac{1}{\omega_0 C_{SC\_b}}I(D1'T)\sin\omega_0 t_2\right), \quad (2.4)$$

where: $0 < t_2 < (1-D1')T$ is time counted from the moment when loop II closes, s.

In a similar way, the operation of ESS can be described in the boost mode. When VT2 is conducting, current loop II is closed, and *i* and v_C values are determined by the equations:

$$i(t) = e^{-bt}\left(-V_C(0)\frac{1}{\omega_0 L}\sin\omega_0 t + I(0)\left(\cos\omega_0 t - \frac{b}{\omega_0}\sin\omega_0 t\right)\right), \quad (2.5)$$

$$v_C(t) = -e^{-bt}\left(-V_C(0)\left(\cos\omega_0 t + \frac{b}{\omega_0}\sin\omega_0 t\right) - \frac{1}{\omega_0 C_{SC\_b}}I(0)\sin\omega_0 t\right), \quad (2.6)$$

where: *0<t<D2'*T — time counted from the beginning of period, s;

D2' — VT2 duty cycle.

When VT2 is switched off, current loop I is closed, and the following equations are valid:

$$i(t_2) = e^{-bt_2}\left((V_{in} - V_C(D2'T))\frac{1}{\omega_0 L}\sin\omega_0 t_2 + I(D2'T)\left(\cos\omega_0 t_2 - \frac{b}{\omega_0}\sin\omega_0 t_2\right)\right), \quad (2.7)$$

$$v_C(t_2) = U_{in} - e^{-bt_2}\left((V_{in} - V_C(D2'T))\left(\cos\omega_0 t_2 + \frac{b}{\omega_0}\sin\omega_0 t_2\right) - \frac{1}{\omega_0 C_{SC\_b}}I(D2'T)\sin\omega_0 t_2\right), \quad (2.8)$$

where: *0<t₂<(1-D2')T* is time counted from the moment when loop I closes, s.

To ensure the correct operation of the analytic model in the buck mode, it is sufficient to calculate *i(t)* and $v_C(t)$ only at $t = D1T$ for equations (2.1) and (2.2) and $t_2 = (1 - D1')T$ for (2.3) and (2.4). If SC current control circuit is introduced, additional calculation at $t = D1'T/2$ for (2.1) is required.

Similarly, the boost mode requires solving (2.5), (2.6) at $t = D2'T$ and (2.7), (2.8) at $t_2 = (1-D2')T$.

Simulation Results

Based on these equations, an analytic ESS model in *Matlab/Simulink* was created. The model uses the controlled current source, which is controlled by an algorithm that determines the execution sequence of equations (2.1)–(2.8).

Fig. 2.11 shows current waveforms for ESS analytic and switching models (switching model contains the circuit shown in Fig. 2.10 and PWM modulator). In this example, the switching period of DC/DC converter is assumed to be 1 kHz. To ensure the precise operation of switching model, simulation time step in *Simulink* must be set to 1 μs, which leads to 75 times longer simulations if compared to simulations carried out by the analytic model.
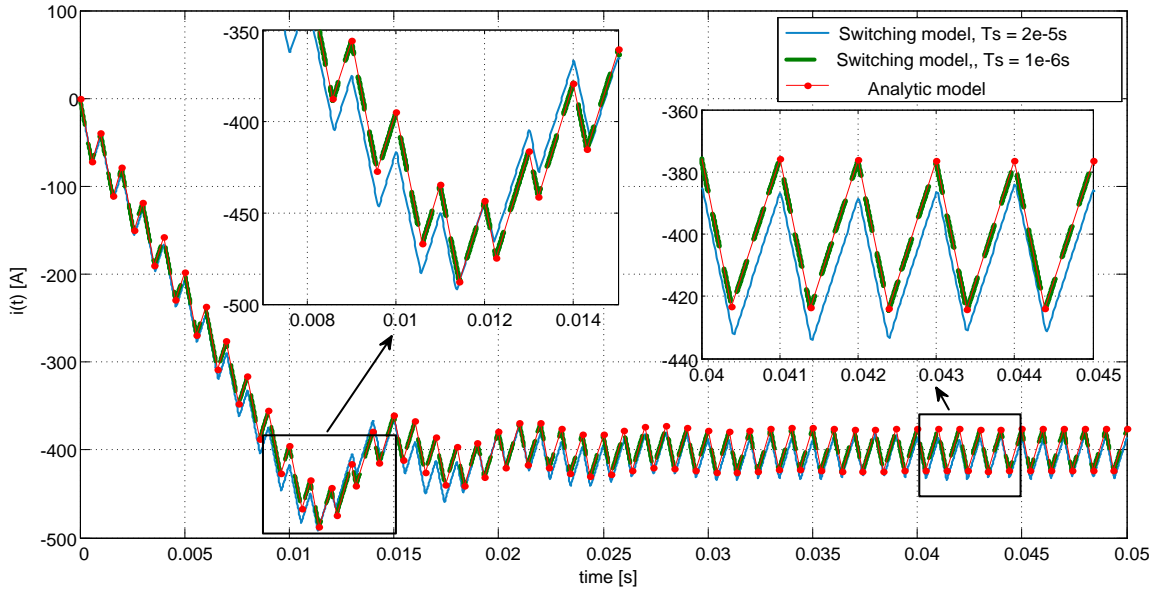
Fig. 2.11. Current waveform comparison for switching and analytic models.

3. Method for Choosing Optimal Number of Supercapacitors for Energy Storage System

3.1. Method for Energy Storage System Profit Maximisation

The method contains 5 stages, and it can be used for stationary and mobile ESS. The method will be explained using it in an example, where optimal parameters are determined for ESS, which could be installed in Riga 8th traction substation.

Stage 1

The energy amount that can be recovered within a year $E_{recoverable\_y}$ using ESS with different maximum power P_{ESS} and energy capacity E_{ESS} parameters must be calculated. A convenient and fast way of doing this is by using stochastic modelling [44]. Stochastic modelling in this case is based on experimentally measured tram diagrams within the feeding area of 8th substation, and the results of it can be seen in Fig. 3.1.
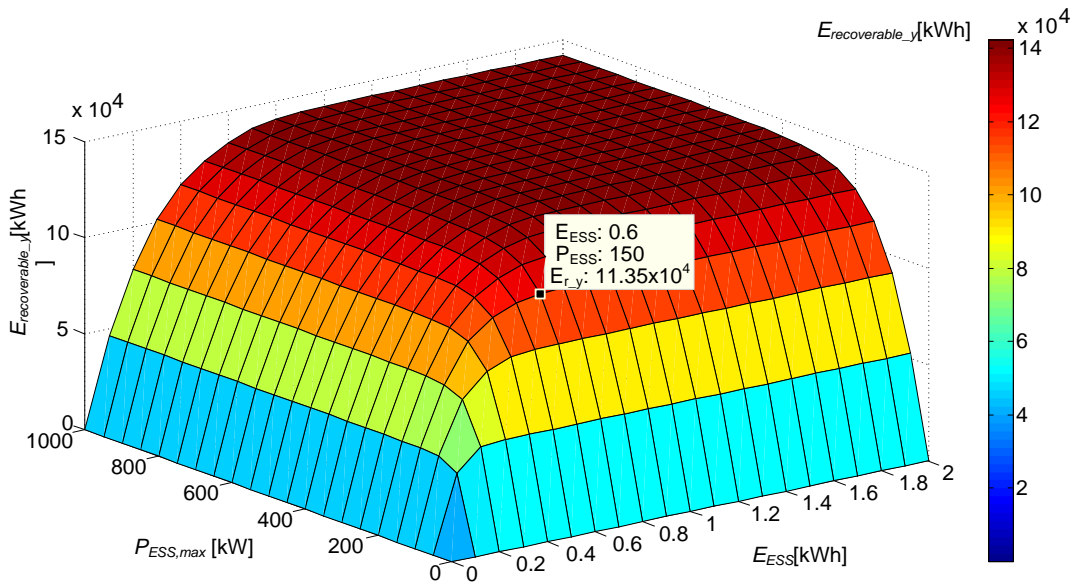

Fig. 3.1. Energy amount that can be recovered in Riga 8th traction substation within a year.

Stage 2

ESS and SC parameters are linked by equations:

$$E_{\text{ESS}} = N \cdot \frac{C_{\text{SC}} \cdot V_{\text{SC,max}}^2}{2} \cdot \left(1 - d^2\right), \tag{3.1}$$

$$P_{\text{ESS,max}} = N \cdot d \cdot V_{\text{SC,max}} \cdot I_{\text{SC,max}}, \tag{3.2}$$

where N — number of SCs in SC bank, pieces;

$d = V_{\text{SC,min}}/V_{\text{SC,max}}$ — SC discharge level;

$V_{\text{SC,max}}$ — maximum SC voltage, V;

$V_{\text{SC,min}}$ — minimum SC voltage, V;

C_{SC} — capacitance of a single SC cell, F;

$I_{\text{SC,max}}$ — maximum SC current, A.

Using (3.1) and (3.2), equations that define the minimum number of SCs and their discharge level, which satisfies particular ESS power and energy parameters, can be derived:

$$N = N_{\min} = \frac{E_{\text{ESS}}}{V_{\text{SC,max}}^2 C_{\text{SC}}} + \sqrt{\left(\frac{E_{\text{ESS}}}{V_{\text{SC,max}}^2 C_{\text{SC}}}\right)^2 + \left(\frac{P_{\text{ESS,max}}}{V_{\text{SC,max}} I_{\text{SC,max}}}\right)^2}, \tag{3.3}$$

$$d = d_{\text{opt}} = \sqrt{\left(\frac{E_{\text{ESS}} I_{\text{SC,max}}}{P_{\text{ESS,max}} V_{\text{SC,max}} C_{\text{SC}}}\right)^2 + 1} - \frac{E_{\text{ESS}} I_{\text{SC,max}}}{P_{\text{ESS,max}} V_{\text{SC,max}} C_{\text{SC}}}. \tag{3.4}$$

Equations (3.3) and (3.4) are used to perform SC battery sizing, and the results are shown in Fig. 3.2. Sizing is based on SC cells with $C_{\text{SC}} = 3400$ F and $V_{\text{SC,max}} = 2.85$ V. SC cycling with high current leads to a very fast decrease in their capacitance [45];, therefore, here $I_{\text{SC,max}}$ is assumed to be 100 A, which matches the current value used by SCs manufacturers for SC cycle life estimation.
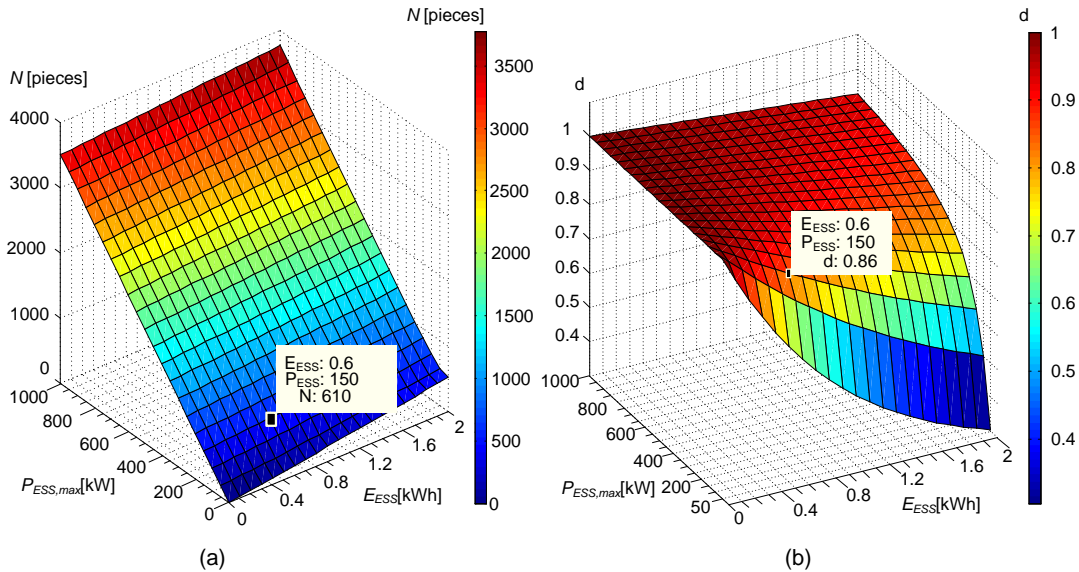

Fig. 3.2. SC battery parameters: (a) number of SCs; (b) SC discharge level.

Stage 3

In this stage, the cost of ESS installation is estimated. As the input parameter in this stage the number of SCs determined by stage 2 is used.

Estimation of SC battery price is relatively easy, because SCs are produced by many manufacturers and the price for different number of SCs can be found on the Internet. The second part of ESS is DC/DC power converter. Since DC/DC converter for such application must be customised, it is very hard to estimate its price. Another part of ESS installation cost that is hard to estimate is expenditures for system installation. Therefore, in this method the price of ESS installation K_{ESS} is calculated by the following equation:

$$K_{\text{ESS}}(P_{\text{ESS,max}}, E_{\text{ESS}}) = N \cdot K_{\text{SC}} \cdot k, \tag{3.5}$$

where N — number of SCs, pieces;

K_{SC} — price for one SC, EUR;

k — ESS price coefficient that allows taking into account DC/DC converter price and expenditures related to the production and installation of ESS.

An approach where ESS price is calculated by (3.5) is also used by other authors [22]. Besides they assume that $k = 2$.

In our example, we will assume that $k = 2$ and $K_{\text{SC}} = 50$ EUR. The results of ESS price calculations are shown in Fig. 3.3.
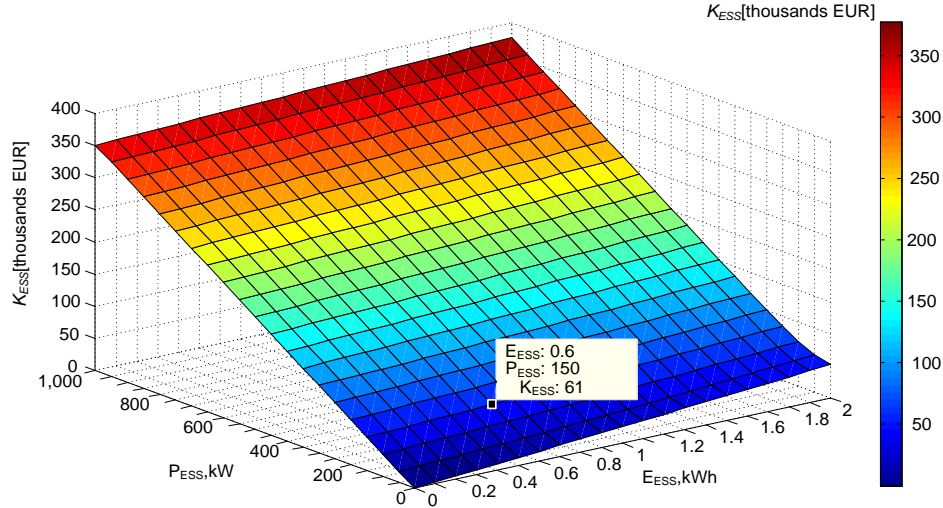

Fig. 3.3. Price of ESS with various power and energy capacity parameters.

Stage 4

Net present value of electrical energy that will be saved with ESS in its operation life time is calculated:

$$PV\left(z, T_{\text{SC\_m}}\right) = \sum_{t=0}^{t=T_{\text{SC\_m}}} \frac{E_{\text{recoverable\_y}}\left(E_{\text{ESS}}, P_{\text{ESS,max}}\right) K_{\text{el}}}{\left(1+z\right)^{t}}, \tag{3.6}$$

where z — discount rate, %;

$T_{\text{SC\_m}}$ — SC lifetime, years;

$E_{\text{recoverable\_y}}(E_{\text{ESS}}, P_{\text{ESS,max}})$ — energy that can be recovered in a year, kWh;

K_{el} — electrical energy price, EUR/kWh;

t — year that is being calculated.

As SC manufacturers in their datasheets say that typical SC lifetime is 10 years, we will use this number for PV calculation in our example. We will assume that the price of electrical energy is 0.1 EUR/kWh and $z = 5$ %.
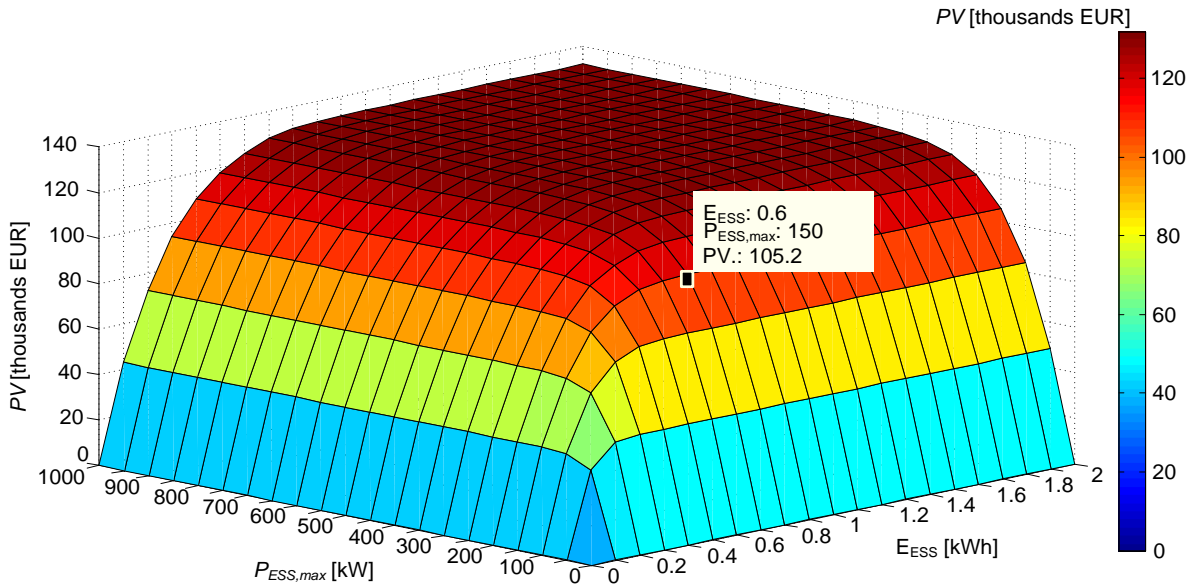
Fig. 3.4. Net present value of recoverable electrical energy in the 8th substation.

Stage 5

Potential profit of ESS installation is determined by subtracting ESS installation costs (stage 3 results) from net present value of recoverable energy (stage 4 results).

Surface area (see Fig. 3.5), which is coloured in blue, shows parameters of ESS that would give a negative profit. The maximum point in this diagram is at $P_{ESS,max} = 150$ kW and $E_{ESS} = 0.6$ kWh. Installation of ESS with such parameters would result in 44,000 EUR profit. It would contain 610 SCs with a discharge level of 0.86. Expenditures associated with ESS installation would be 61,000 EUR, and such ESS would recover approximately 113 MWh of electrical energy every year.
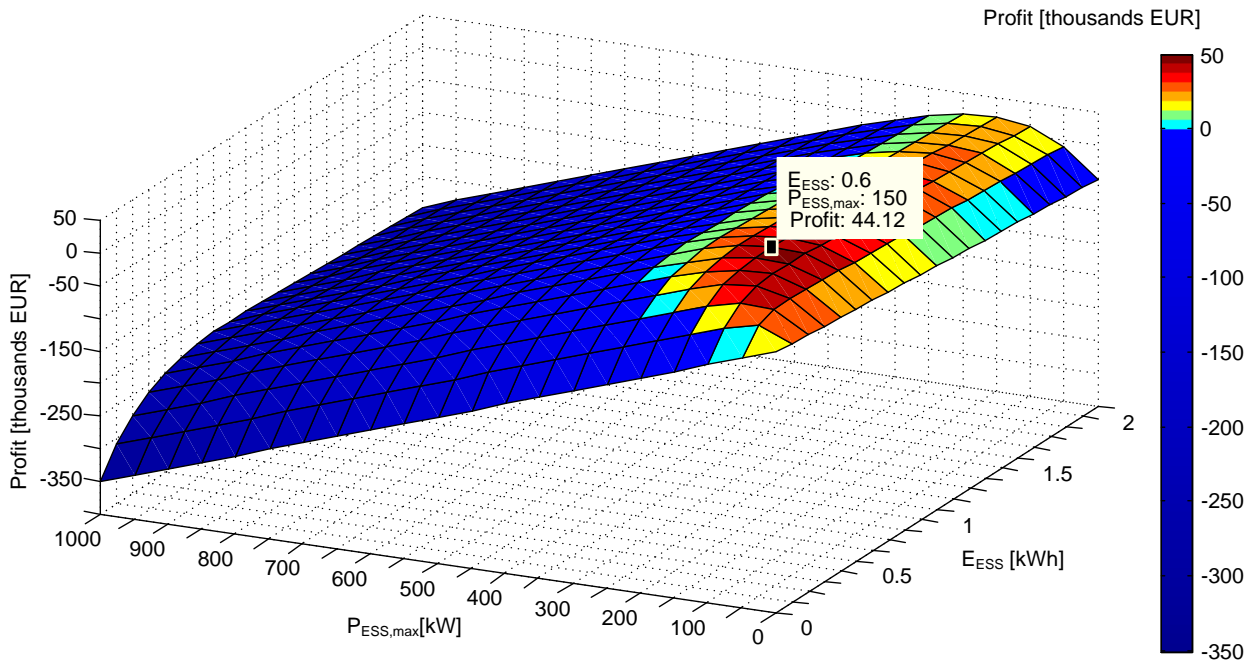

Fig. 3.5 Potential profit of various parameter ESS installation in the 8th substation.

3.2. Application of Method for Mobile Energy Storage System

The previously described method was used to find optimal parameters for mobile ESS. Potential profit of ESS installed on tram T3A is shown in Fig. 3.6.
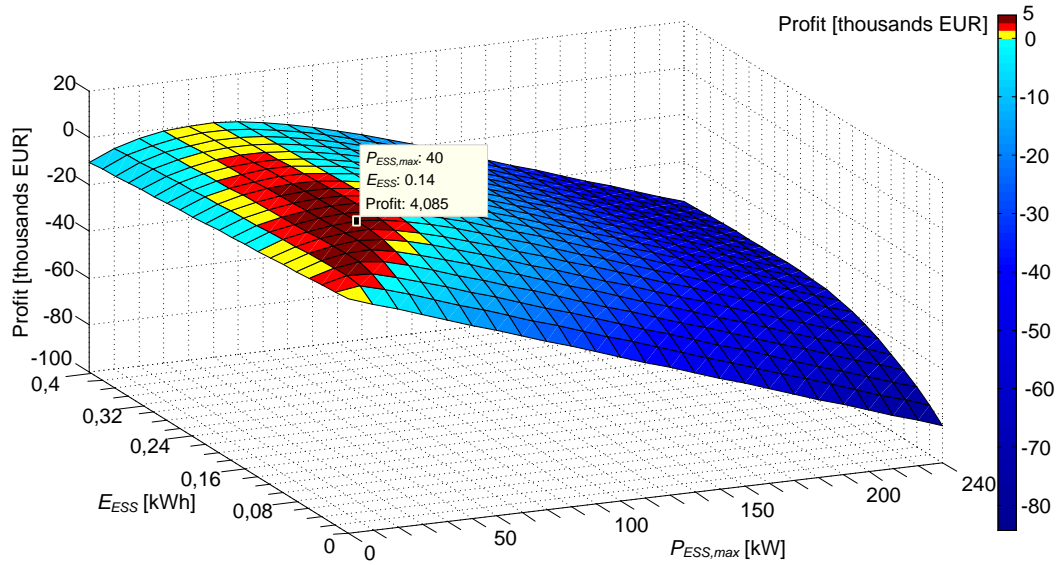
Fig. 3.6. Potential profit of various mobile ESS installed on tram T3A ($I_{SC,max} = 100$ A, $C_{SC} = 3400$ F, $V_{SC,max} = 2.85$ V, $K_{el} = 0.1$ EUR/kWh, $z = 5$ %).

As can be seen, maximum profit is 4,085 EUR, and it can be achieved with ESSs that have $P_{ESS,max} = 40$ kW and $E_{ESS} = 0.14$ kWh. Such ESS would contain 160 SCs.

In the proposed method, the ESS power capability is assumed to be constant; however, in practical implementation maximum current is constant and power capability depends on SC state of charge. Therefore, a diagram of net present value of the ESS as a function of number of SC cells and discharge coefficient is obtained (Fig. 3.7) taking into account also the losses due to SC internal resistance and the constant maximum current. As can be seen from the diagram, a point of 160 cells and discharge coefficient 0.87 give just by 22 EUR less ESS net present value than maximum point with 150 cells and the same discharge coefficient. From that we can conclude that the optimum (160 cells and discharge coefficient 0.87) obtained with the proposed method practically allows choosing the best parameters for a particular ESS application.
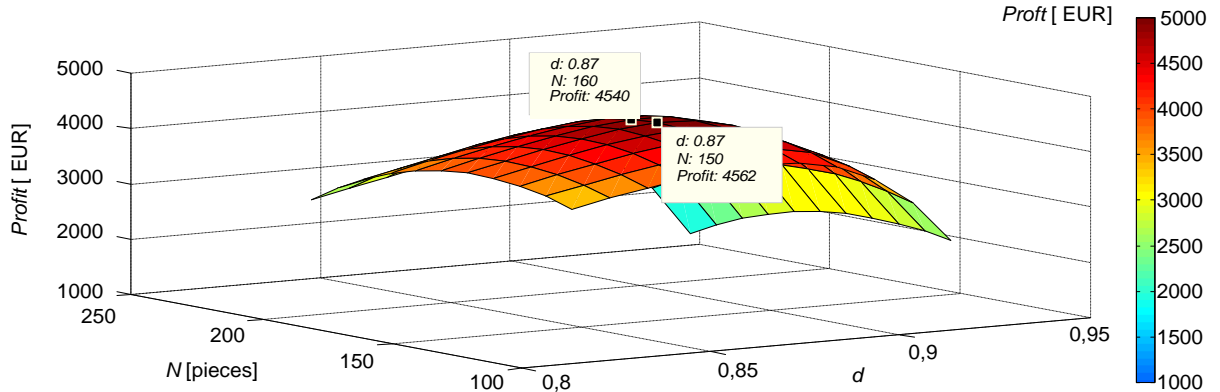

Fig. 3.7. Potential profit of mobile ESS installed on tram T3A taking into account SC losses.

4. Effect of Energy Storage System Control Parameters on System Performance

4.1. Analysis of Mobile Energy Storage System Parameters

Installation of ESS aboard the electrical vehicle is the most efficient way to save its regenerative braking energy. Only an on-board ESS provides the braking energy storage at the place of its generation and the direct use of stored energy at the place of its consumption. However, this is also the most expensive way of saving braking energy, because each ESS serves only one tram.

Therefore, it is important to carefully choose the number of SCs and control ESS wisely in order to operate ESS in the most efficient way.

Analysis of Mobile ESS Parameters Using an Idealised Power Diagram

In this chapter, ESS parameters are analysed for trolleybus Skoda 24Tr. It is assumed that 17 t heavy trolleybus brakes with constant deceleration ($2 m/s^2$) and its initial speed is 50 km/h. If kinetic energy during braking is transformed into electrical energy with 50 % efficiency, we obtain a braking profile with the following parameters: maximum braking power $P_{br,max} = 236$ kW; regenerated energy $E_{br} = 820$ kJ.

ESS Operation Modes

Fig. 4.1 shows the block diagram of a vehicle that is equipped with ESS and is in the braking mode. DC/DC converter with efficiency η ensures the controlled energy flow from a vehicle to an SC battery.
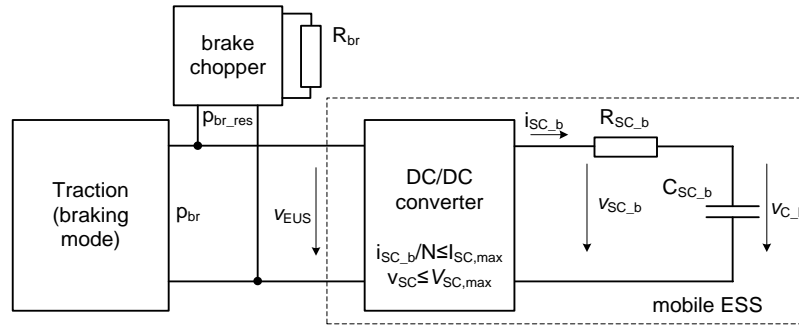

Fig. 4.1. Block diagram of a trolleybus that is equipped with ESS.

Fig. 4.2 displays the operational diagrams for the case of a vehicle with braking power p_{br} that linearly decreases from $P_{br,max}$ to 0 in the time interval $0-t_{br}$. In general, three modes of the ESS operation can be distinguished:

- charging1 — takes place within the interval $0-t_1$ when braking power p_{br} exceeds the ESS power capability restricted by current limitation. In this mode, braking energy is partly dissipated in braking resistors.
- charging2 — normal mode of ESS operation, when all the energy (excluding losses in DC/DC converter and SC battery series resistance R_{SC_b}) is saved in the SC bank.
- charging3 — takes place within the interval t_2-t_3 and is a mode of SC battery voltage stabilisation at the level $v_{SC\_b} = const = V_{SC\_b,max}$.
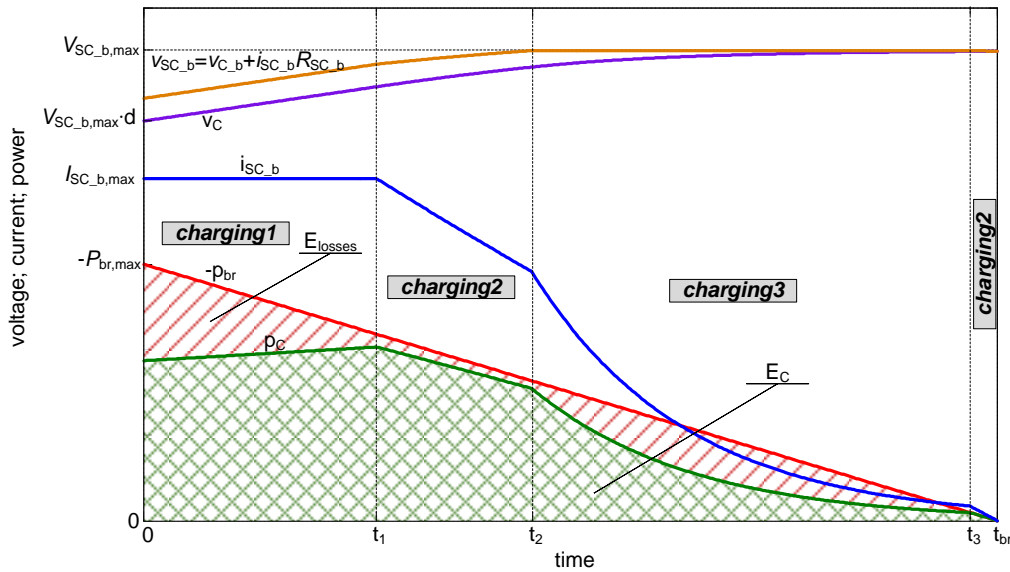

Fig. 4.2. Mobile ESS operation modes.

SC Battery Sizing Considerations

In order to ensure that braking energy is not dissipated in brake resistors, the following inequalities must be satisfied:

$$E_{ESS} \geq E_{br}; P_{ESS,max} \geq P_{br,max}. \qquad (4.1)$$

Inserting (4.1) in (3.1) and (3.2), we obtain inequalities that determine the number of SCs:

$$N \geq \frac{2E_{br}}{V_{SC,max}^2 C_{SC}(1-d^2)}, \qquad (4.2)$$

$$N \geq \frac{P_{br,max}}{V_{SC,max} I_{SC,max} d}. \qquad (4.3)$$

Fig. 4.3 shows how number of SCs is affected by the discharge level at different $I_{SC,max}$ values. Curves are obtained with (4.2) and (4.3) using the following input data: $E_{br} = 820$ kJ, $P_{br,max} = 236$ kW, $C_{SC} = 3400$ F and $V_{SC,max} = 2.85$ V. Equation (4.2) is used to obtain curve $N(E_{br})$, which takes into account only ESS energy capacity.
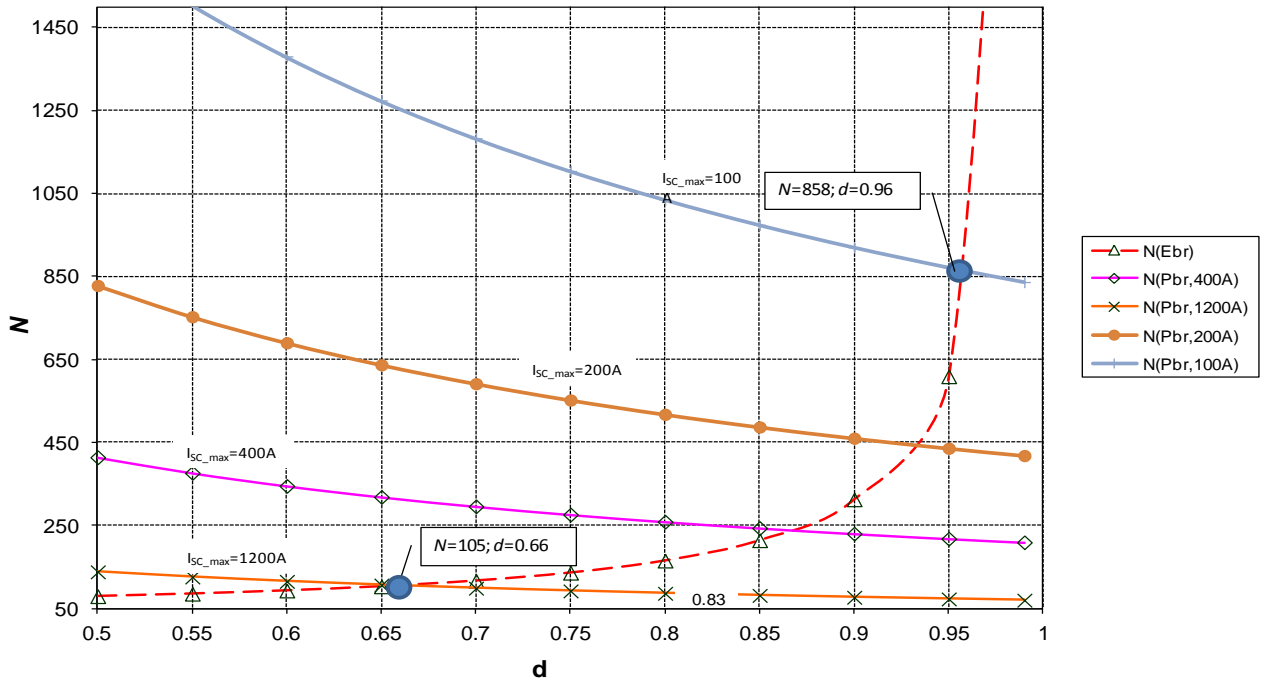

Fig. 4.3. Number of SCs vs. discharge level at different maximum SC current values.

The solid lines in Fig. 4.3 are calculated according to (4.3) for $I_{SC,max} = 100; 200; 1200$ A; and 576 A, and show the necessary number of SCs taking into account the power requirements. The last value ($I_{SC,max} = 1200$ A) is chosen equal to $0.12 I_{ShortCircuit}$ recommended in [46], [47], [48] as the maximum current allowed for SCs. The chosen N value should be located above both the energy and the power curves. The point of intersection gives the minimum N and the optimum d values meeting both the energy and the power requirements. These values can be calculated by (3.3) and (3.4). If $I_{SC,max} = 1200$ A is chosen, 105 SCs, with $d = 0.66$, are sufficient to ensure that all recoverable braking energy is saved. If $I_{SC,max}$ is set to 100 A, all recoverable braking energy can be saved with 858 SCs with discharge level 0.96. In the considered $I_{SC,max}$ range 100–1200 A, the optimum d value is higher than 0.66, which does not match $d = 0.5$, which is often used in research dedicated to SC battery sizing.

Mobile ESS Parameter Analysis Using Experimentally Measured Power Diagrams

To find out how mobile ESS affects energy consumption from a substation, a more realistic situation was studied. In this study, experimentally measured 19 hour-long tram T3A power diagram was used as input data for a mathematical model of the system, which is shown in Fig. 4.4. In such a simplified system, V_sub can be viewed as a constant DC voltage source that provides power only in one direction. R_l includes electrical resistance of overhead contact lines, rails and feeding cables. Since trams are continuously in motion, the value of R_l is alternating, but for simplification it is assumed that the average value of R_l is 0.05 Ω. The character of the tram is determined by its power (p_{tr}). If p_{tr} has positive values, the tram is in the running mode and is viewed as a load, whereas negative p_{tr} values determines that the tram operates as a power generator. ESS positive power values will be associated with SC charging, while negative values — with discharging.

In the discharging state, ESS has 2 operation modes:

- discharging1 — ESS delivers the power to the tram according to the equation:

$$p_{ESS} = k_p \cdot p_{tr}, \qquad (4.4)$$

where k_p — discharge power proportionality coefficient;

- discharging2 — requested power from ESS exceeds its power and ESS power is limited to:

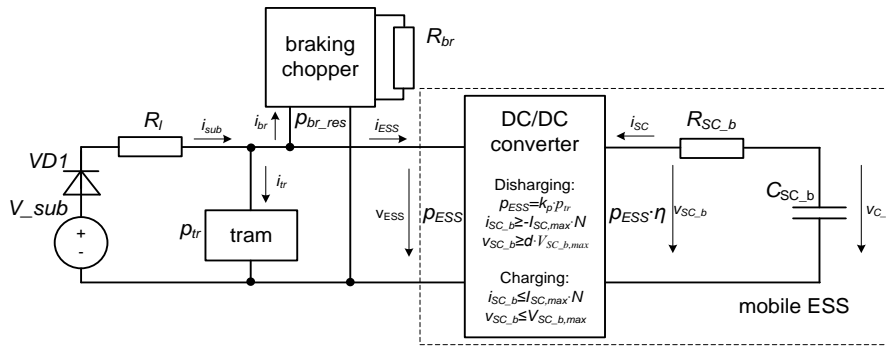$$p_{ESS} = I_{SC\_b,max} \cdot v_{SC\_b} \cdot \eta. \qquad (4.5)$$

Fig. 4.4. Block diagram of a tram feeding infrastructure and tram equipped with mobile ESS.

The parameters that can affect ESS operation are d and k_p. These parameters will be changed in a wide range in order to find their optimum combination, which gives the best results. Besides, k_p and d values will be selected before each simulation and during simulation will remain constant. Therefore, this ESS control method will be called "constant parameter method". Results of simulations will be evaluated in a relative unit that shows by what percentage the energy consumption from a substation has decreased compared to a situation when there is no ESS:

$$E_{sub\_r} = \frac{E_{sub0} - E_{sub}}{E_{sub0}} 100\ \%, \qquad (4.6)$$

where E_{sub0} — energy consumption from a substation when a tram is not equipped with ESS;

E_{sub} — energy consumption from a substation when a tram is equipped with ESS.

To reduce the amount of energy that is wasted in brake resistors when ESS operates in charging1 or charging3 mode, SC bank before every braking should be discharged to the level, which allows storing exactly the amount of energy that will be recuperated. This means that maximum power capability and sufficient energy capacity of ESS for a particular braking profile will be provided. To carry out the ESS operation analysis with such a control method, a tram power diagram must be divided into sections, where the length of each section is determined by the time that tram is in motion. The section starts when the tram starts to accelerate and ends when the speed of the tram decreases to 0 km/h. An example of tram power profile in one such section is depicted in Fig. 4.5.
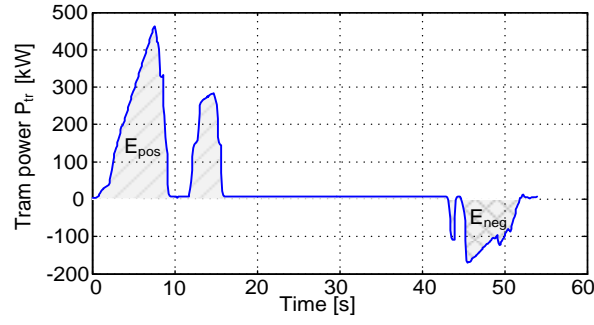
Fig. 4.5. Tram power diagram that shows one acceleration and one braking.

Since the energy amount that the tram will consume (E_{pos}) and recuperate (E_{neg}) in each power diagram section is known, it is possible to calculate the discharge level of SC bank and proportionality coefficient of discharge power according to equations:

$$d = \frac{\sqrt{V_{SC\_b,max}^2 - \dfrac{2E_{neg}}{C_{SC\_b}}}}{V_{SC\_b,max}^2}, \tag{4.7}$$

$$k_p = \frac{E_{neg}}{E_{pos}}. \tag{4.8}$$

This control method, where control parameters are calculated for each tram braking event, will be called a "variable parameter method". Nonetheless, it is impossible to implement the second control method for ESS in real application, it can be used for comparative evaluation of the constant parameter control method.

Simulation Results

Mathematical model of the system shown in Fig. 4.4 is developed in *Matlab*. The model contains equations that describe electrical parameters of this system and the algorithm, which controls the execution sequence of these equations and changes the value of parameter that is being studied.

Fig. 4.6 illustrates simulation results, where a constant parameter control method was tested (C_{SC} = 3400 F, $V_{SC,max}$ = 2.85 V, $I_{SC,max}$ = 100 A). In these simulations, SC battery size was changed and for each k_p value optimal d was found. As it can be seen, changing k_p value in the range from 0.3 to 1 leaves very small effect on E_{sub_r}. If the value of k_p is chosen lower than 0.3, E_{sub_r} decreases rapidly. For example, if we choose N = 500 and change k_p from 0.3 to 1, E_{sub_r} decreases only by 0.5 %, whereas k_p value 0.2 leads to approximately 3 % increase in energy consumption from a substation. Simulation results depicted in Fig. 4.6 also show how E_{sub_r} is affected by the size of SC battery. As it can be seen, choosing ESS with N higher than 500 is not necessary because it has a very little effort on E_{sub_r}. Changing N from 500 to 800 increases E_{sub_r} only by 2 %.
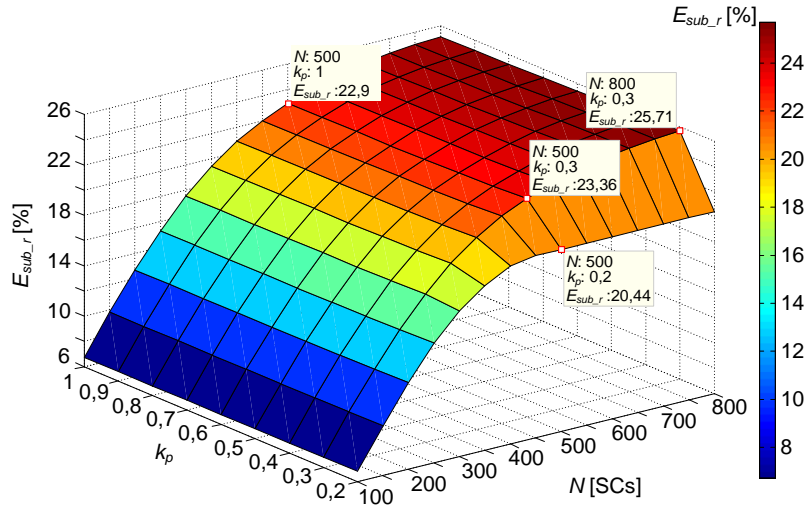
25

Fig. 4.6. Reduction in energy consumption from a substation with various ESSs.

Fig. 4.7 shows how SC discharge level influences E_{sub_r} with various sized SC batteries. The best results are achieved if d value is set to 0.87. Choosing d under this value increases the losses due to ESS operation in charging1 mode, while d values larger than 0.87 lead to additional losses due to charging3 mode.
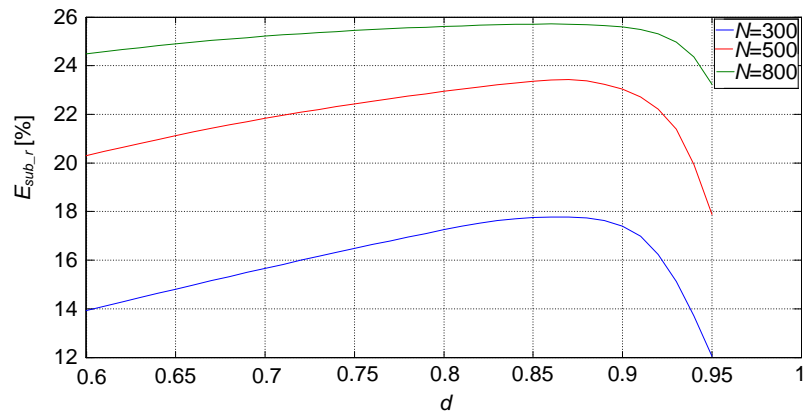
Fig. 4.7. ESS discharge level effect on substation energy consumption.

To evaluate the efficiency of a relatively simple constant parameter control method, it was compared with variable parameter control method, and the results are shown in Fig. 4.8. As can be seen, the variable parameter control method on average gives only 0.5 % better results than constant parameter method with $k_p = 0.3$ with the corresponding optimum d value.

Fig. 4.8. ESS control method comparison (parameters for constant parameter method:
$k_p = 0.3$, $d = d_{opt}$).

4.2. Analysis of Stationary Energy Storage System Control Parameters

To find out how ESS control parameters affect energy consumption from a substation, these parameters must be changed in a wide range, which means that numerous simulations must be performed. Since a 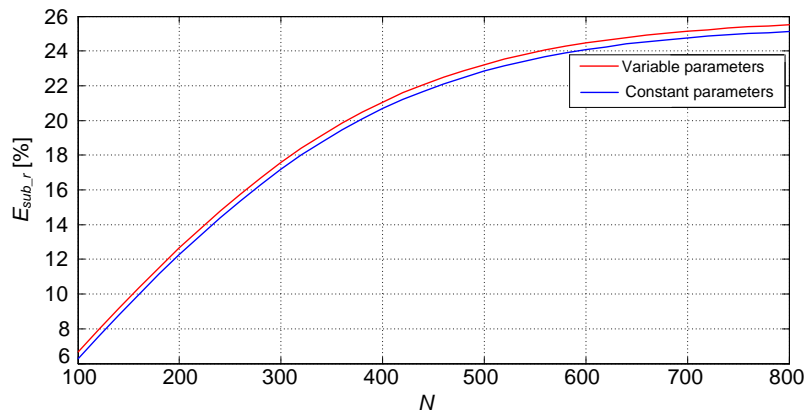tram system simulation model described in the second chapter of the present research requires relatively small simulation step size, it cannot be used for this purpose. Therefore, a simplified mathematical model of tram system is made and its block diagram is shown in Fig. 4.9. The main elements here are stationary SCs based ESS, substation, contact line resistance and tram.
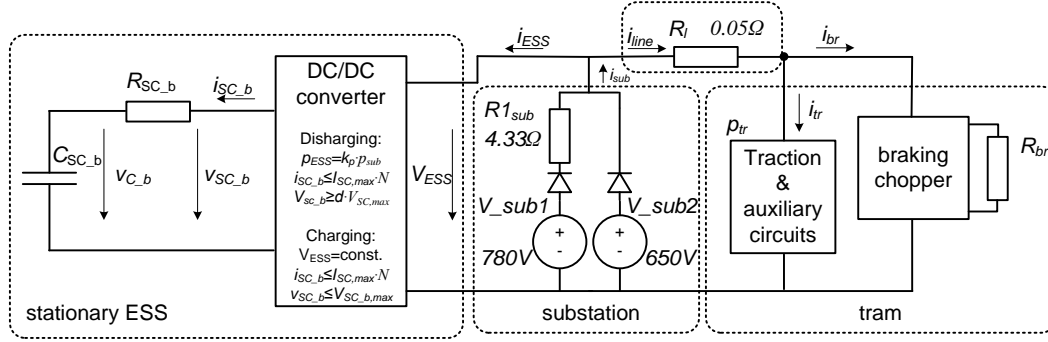

Fig. 4.9. Simplified block diagram of tram system equipped with stationary ESS.

As this model contains only one tram block, for simulation of multiple trams power diagrams are synthesized from experimentally measured power diagram of one tram.

Stationary ESS in this study contains DC/DC converter and SC battery, which contains 800 SCs (capacitance of one SC is assumed to be 3400 F). During charging, DC/DC converter can operate in 3 modes:

- charging1 — stationary ESS is in the normal operation mode and stabilizes the input voltage of ESS (V_{ESS}) to some pre-set value;

- charging2 — the braking power of trams is too high and SC bank charging current i_{SC_b} is limited to the value that corresponds to maximum permissible single SC cell current value $I_{SC,max}$, which here is assumed to be 100 A;

- charging3 — the voltage over the SC battery reaches the maximum permissible value; therefore, SC battery current is limited to :

$$i_{\mathrm{SC\_b}} = \frac{V_{\mathrm{SC\_b,max}} - v_{\mathrm{C\_b}}}{R_{\mathrm{SC\_b}}}. \tag{4.9}$$

In the running mode of tram, ESS has to discharge the energy it stores. The energy from ESS is discharged proportionally to substation power p_{sub}. In the discharge state, ESS has 2 operation modes:

- discharging1 — ESS is discharged with power that is proportional to substation power p_{sub}

$$p_{\mathrm{ESS}} = k_p \cdot p_{\mathrm{sub}}, \tag{4.10}$$

where k_p — proportionality coefficient;

- discharging2 — ESS power is limited to the level, which ensures that SC current is not exceeding 100 A.

ESS Control Parameters and Simulation Results

SCs discharge level is a variable, which influences the ESS operation in discharging and charging modes. Choosing low d values increases the energy capacity of ESS, but decreases its power capability, which leads to ESS operation in charging2 mode. On the other hand, if too high d values are chosen, ESS energy capacity is not sufficient and ESS operates in charging3 mode.

The second ESS control parameter that will be studied in these simulations is the input voltage of ESS V_{ESS}. In the braking mode, higher V_{ESS} values decrease the substation power that charges SCs

and ensures that the power from a tram is transferred to ESS via a higher voltage level, which means that resistive losses in R_l are decreased. On the other hand, too high V_{ESS} values lead to situations where not all braking energy is passed to ESS because the maximum power that can be transferred from a tram to ESS is limited by equivalent resistance of contact lines and feeding cables:

$$P_{\text{line\_max}} = \frac{(V_{\text{br\_max}} - V_{\text{EUS}})V_{\text{br\_max}}}{R_l}, \quad (4.11)$$

where $V_{\text{br\_max}}$ — braking chopper actuation voltage (780 V).

In order to examine how the above-mentioned ESS control parameters influence ESS operation efficiency, numerous simulations were carried out for different number of trams, and the obtained results are shown in Fig. 4.10.

Four data points in Fig. 4.10 for the case with 1 tram are highlighted to show how $E_{\text{sub\_r}}$ value changes when d and V_{ESS} are varied in a range between 0.7–0.9 and 700–765 V, respectively. As can be seen, the change in the value of V_{ESS} has very small effect on $E_{\text{sub\_r}}$. This means that the difference of energy amount that is charged in SCs from a substation and the difference of energy that is lost in R_l at different V_{ESS} values are negligible. V_{ESS} influences value of $E_{\text{sub\_r}}$ only if its value is increased over 765 V and saved energy is affected by contact line resistance according to (4.11). Similar V_{ESS} effect on $E_{\text{sub\_r}}$ can be observed also for a higher number of trams. At V_{ESS} = 765 V, approximately 1.5 % of energy charged in ESS was coming from a substation.
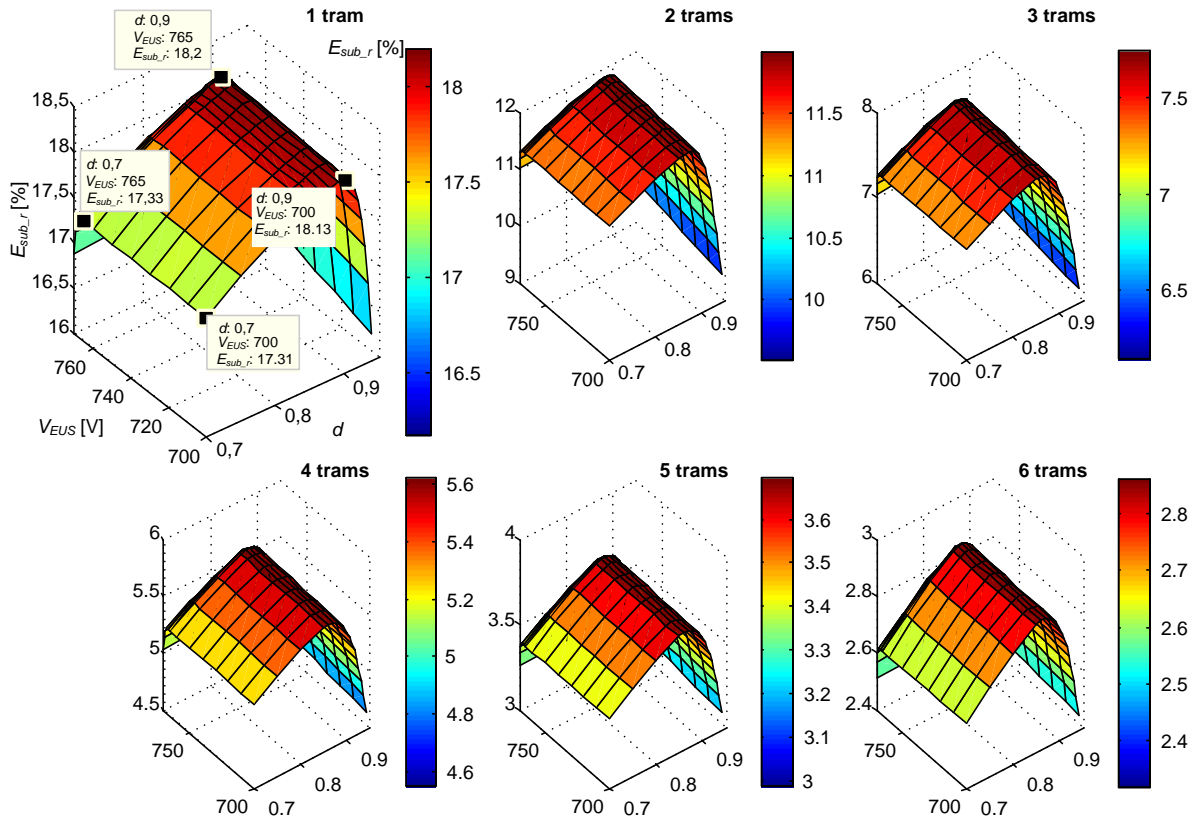

Fig. 4.10. Reduction in energy consumption from a substation with different ESS control parameters.

Fig. 4.10 also shows that $E_{\text{sub\_r}}$ decreases as the number of trams increases. In the case of one tram, maximum $E_{\text{sub\_r}}$ is 18.2 %, while in the case of 6 trams $E_{\text{sub\_r}}$ is only 2.86 %.

More detailed d effect on $E_{\text{sub\_r}}$ is shown in Fig. 4.11, where energy consumption is analysed for fixed ESS input voltage value (V_{ESS} = 765 V). Analysis of these results leads to a conclusion that the value of d for ESS can be held constant for any number of trams and this value should be 0.86 or 0.87. Although this is not the optimum point for the case of 1 tram, $E_{\text{sub\_r}}$ difference is too small to be considered.
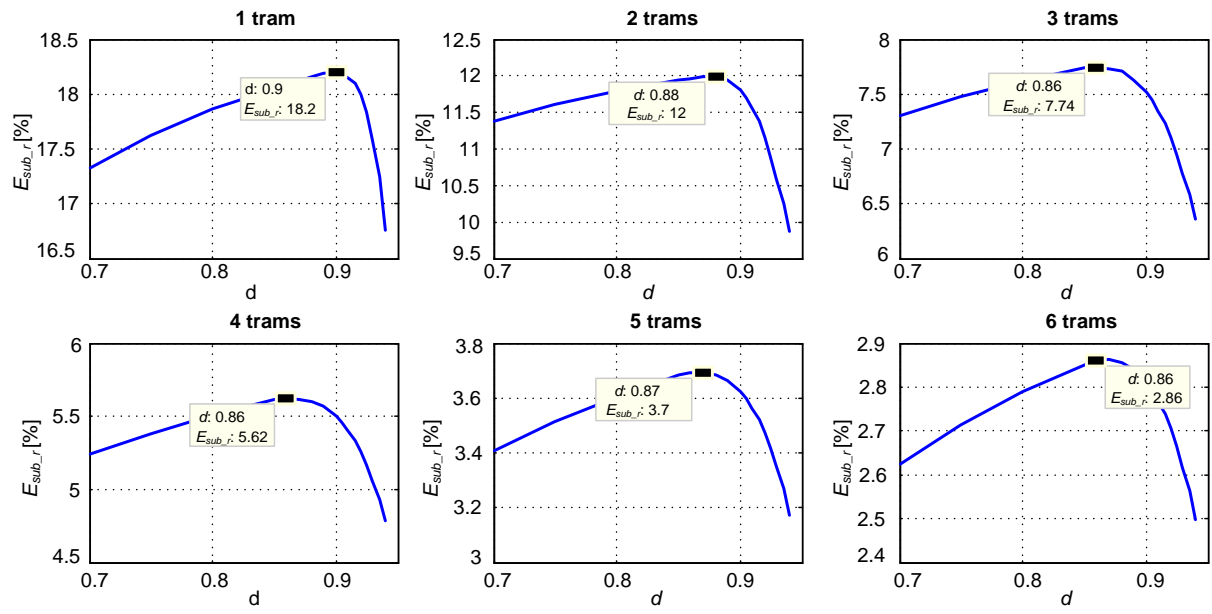
Fig. 4.11. Reduction in energy consumption from a substation with different *d* values.

Conclusions

Since SCs with good power parameters are available for about 15 years, research on their usage in ESSs with the goal to save braking energy of urban electric transport is very topical. Besides, only few SCs based ESSs are installed in real urban electric transport systems.

There are four main technologies that can be used to recover braking energy: reversible substations, flywheels, SCs and electrochemical accumulators. The least commercialised technology is flywheel based energy storage systems, which can be explained by complexity of these systems.

The proposed method for obtaining an equivalent electrical circuit of overhead contact lines of urban electric transport allows obtaining a significantly simplified overhead contact line circuit. This simplified circuit can be used to evaluate a voltage drop in various overhead contact line points.

The developed *Matlab/Simulink* model of a tram system can be used to analyse energy consumption in various system elements. If high computing power is available, this model can be used for optimisation of ESS power and control parameters.

Analytic current and voltage equations of series connected RLC circuit can be used to describe the operation of energy storage system, which is made of buck & boost converter and SC battery. Mathematical model, which uses these equations, significantly shortens the time needed for simulation of such a system.

The proposed method for choosing ESS power and energy parameters shows that the number of SCs in ESS for transport systems in flat terrain is mainly determined by SC power capability. By applying the proposed method for Riga 8th traction substation, it can be seen that installing ESS in this substation can be profitable. Application of this method for mobile and stationary ESS sizing also shows that optimally sized ESS ensures only partial recovery of braking energy.

If a traction substation, which uses a six-phase rectifier with an interphase transformer, is equipped with ESS, approximately 1.5 % of energy in such ESS will be charged from a substation.

If mobile ESS is discharged with the power that is proportional to substation power, proportionality coefficient should be at least 0.3, to ensure that ESS will have a sufficient energy capacity for next braking event.

The proposed voltage measuring system for series connected SCs cells can be used for research where SCs are tested in a wide voltage range.

References

[1] European Commission, "Europe2020: A Strategy for Smart, Sustainable and Inclusive Growth". 2010.

[2] Rīgas Dome, "Riga Smart City Sustainable Energy Action Plan for 2014–2020". 2014.

[3] L. Latkovskis, L. Grigans, U. Sirmelis, and J. Cernovs, "Neizmantotās rekuperētās enerģijas aplēse Rīgas elektriskajā sabiedriskajā transportā", *Latv. J. Phys. Tech. Sci.*, vol. 5, pp. 47–56, 2010.

[4] R. L. Spyker and R. M. Nelms, "Optimization of double-layer capacitor arrays", *IEEE Trans. Ind. Appl.*, vol. 36, no. 1, pp. 194–198, Jan. 2000.

[5] D. MacCurdy, "Public Interest Energy Research (PIER) Program FINAL PROJECT REPORT." 2010.

[6] B. Destraz, P. Barrade, A. Rufer, and M. Klohr, "Study and simulation of the energy balance of an urban transportation network", in *2007 European Conference on Power Electronics and Applications*, 2007, pp. 1–10.

[7] A. Rufer, D. Hotellier, and P. Barrade, "A supercapacitor-based energy storage substation for voltage compensation in weak transportation networks", *IEEE Trans. Power Deliv.*, vol. 19, no. 2, pp. 629–636, Apr. 2004.

[8] R. Barrero, X. Tackoen, and J. Van Mierlo, "Quasi-static simulation method for evaluation of energy consumption in hybrid light rail vehicles", in *IEEE Vehicle Power and Propulsion Conference, 2008. VPPC '08*, 2008, pp. 1–7.[9] R. Barrero, J. Van Mierlo, and X. Tackoen, "Energy savings in public transport", *IEEE Veh. Technol. Mag.*, vol. 3, no. 3, pp. 26–36, Sep. 2008.

[10] R. Barrero, X. Tackoen, and J. Van Mierlo, "Analysis and configuration of supercapacitor based energy storage system on-board light rail vehicles", in *Power Electronics and Motion Control Conference, 2008. EPE-PEMC 2008. 13th,* 2008, pp. 1512–1517.

[11] R. Barrero, X. Tackoen, and J. Van Mierlo, "Improving energy efficiency in public transport: Stationary supercapacitor based Energy Storage Systems for a metro network", in *IEEE Vehicle Power and Propulsion Conference, 2008. VPPC '08*, 2008, pp. 1–8.

[12] R. Barrero, X. Tackoen, and J. Van Mierlo, "Stationary or Onboard Energy Storage Systems for Energy Consumption Reduction in a Metro Network", *Proc. Inst. Mech. Eng. Part F J. Rail Rapid Transit*, vol. 224, no. 3, pp. 207–225, May 2010.

[13] D. I. and D. Lauria, "A New Supercapacitor Design Methodology for Light Transportation Systems Saving", Aug. 2011.

[14] F. Ciccarelli, D. Iannuzzi, and D. Lauria, "Supercapacitors-based energy storage for urban mass transit systems", in *Proceedings of the 2011-14th European Conference on Power Electronics and Applications (EPE 2011)*, 2011, pp. 1–10.

[15] F. Ciccarelli, D. Iannuzzi, and P. Tricoli, "Control of metro-trains equipped with onboard supercapacitors for energy saving and reduction of power peak demand", *Transp. Res. Part C Emerg. Technol.*, vol. 24, no. 0, Oct. 2012, pp. 36–49.

[16] D. Iannuzzi, F. Ciccarelli, and D. Lauria, "Stationary ultracapacitors storage device for improving energy saving and voltage profile of light transportation networks", *Transp. Res. Part C Emerg. Technol.*, vol. 21, no. 1, Apr. 2012, pp. 321–337.

[17] S. D'Avanzo, D. Iannuzzi, F. Murolo, R. Rizzo, and P. Tricoli, "A sample application of supercapacitor storage systems for suburban transit", in *Electrical Systems for Aircraft, Railway and Ship Propulsion (ESARS), 2010*, 2010, pp. 1–7.

[18] D. Iannuzzi, P. Pighetti, and P. Tricoli, "A study on stationary supercapacitor sets for voltage droops compensation of streetcar feeder lines", in *Electrical Systems for Aircraft, Railway and Ship Propulsion (ESARS), 2010*, 2010, pp. 1–8.

[19] F. Ciccarelli, D. Iannuzzi, K. Kondo, and L. Fratelli, "Line Voltage Control based on Wayside Energy Storage Systems for Tramway Networks", *IEEE Trans. Power Electron.*, vol. PP, no. 99, pp. 1–1, 2015.

[20] F. Ciccarelli, D. Iannuzzi, and I. Spina, "Comparison of energy management control strategy based on wayside ESS for LRV application", in *IECON 2013–39th Annual Conference of the IEEE Industrial Electronics Society*, 2013, pp. 1548–1554.

[21] H. Hoimoja, D. Vinnikov, M. Lehtla, A. Rosin, and J. Zakis, "Survey of loss minimization methods in tram systems", in *2010 International Symposium on Power Electronics Electrical Drives Automation and Motion (SPEEDAM)*, 2010, pp. 1356–1361.

[22] H. Hõimoja, "Energy Efficiency Estimation and Energy Storage Calculation Methods for Urban Electric Transportation", Phd Thesis, Tallinn University of Technology, Tallinn, Estonia, 2009.

[23] L. Latkovskis and L. Grigans, "Estimation of the untapped regenerative braking energy in urban electric transportation network", in *Power Electronics and Motion Control Conference, 2008. EPE-PEMC 2008. 13th*, 2008, pp. 2066–2070.

[24] L. Grigans and L. Latkovskis, "Estimation of the power and energy requirements for trackside energy storage systems", in *European Conference on Power Electronics and Applications*, 2009.

[25] A. González-Gil, R. Palacin, P. Batty, and J. P. Powell, "Energy-efficient urban rail systems: strategies for an optimal management of regenerative braking energy", in *Proceedings of TRA2014*, France, p. 9.

[26] T. Knote, "Energy Storage Systems in the Catenary Grid of Light Rail and Trolleybus Systems", Final report Trolley project, 2013.

[27] O. Solis, K. Pham, and D. Turner, "Saving Money Every Day: LA Metro Subway Wayside Energy Storage Sustation", in *Proceedings of 2015 Joint Rail Conference*, USA, San Jose, 2015.

[28] SAFT, "Railway Solutions – Regenerative Hybrid Traction". [Online]. Available: http://www.saftbatteries.com/market-solutions/railways.

[29] "Toshiba Supplies Traction Energy Storage System to Tobu Railway" [Online]. Available: http://www.infotechlead.com/networking/toshiba-supplies-traction-energy-storage-system-tobu-railway-27275.

[30] Hitachi, "Hitachi Review," Vol. 59, No.4, 2010.

[31] "Battery Power System for Railways". [Online]. Available: https://global.kawasaki.com/en/energy/solutions/battery_energy/applications/bps.html.

[32] "Siemens Installing First Regenerative Energy Storage Unit in the U.S. on New TriMet Light Rail Line". [Online]. Available: http://news.usa.siemens.biz/press-release/smart-grid/siemens-installing-first-regenerative-energy-storage-unit-us-new-trimet-lig.

[33] "Increasing Energy Efficiency; Optimized Traction Power Supply in Mass Transit Systems". [Online]. Available: https://w3.siemens.dk/home/dk/dk/mobility/baneelektrificering/Documents/increasing-energy-efficiency_brochure.pdf.

[34] J. Poulin, "An Energy Storage System which Reduces Costs and Generates Revenue for the Transit Authority", presented at the Annual Polis Conference, Spain, Madrid, 2014.

[35] F. Devaux and X. Tackoen, "Overview of braking energy recovery technologies in the public transport field", STIB, 2011.

[36] Maxwell, / Internets. - http://investors.maxwell.com/phoenix.zhtml?c = 94560&p = irol-newsArticle&ID = 1903210.

[37] Meiden, "Annual Report", 2008.

[38] M. Meinert, K. Rechenberg, G. Hein, and A. Schmieder, "Energy Efficient Solutions for the Complete Railway System", in *Proceedings of the 8th World Congress on Railway Research*, Seoul, 2008, pp. P1–P11.

[39] "HESOP; All-in-one Energy & Cost saver". [Online]. Available: http://www.alstom.com/Global/Transport/Resources/Documents/brochure2014/HESOP%20-%20Product%20sheet%20-%20EN%20-%20LD.pdf?epslanguage = en-GB.

[40] "Energy   recovery   systems   for   Bielefeld   tram". [Online].   Available: http://www.ingeteam.com/Portals/0/Catalogo/Sector/Documento/SSE_1381_Archivo_bielefeld-e03.pdf.

[41]   "Energy   recovery   systems   for   Bilbao".   [Online].   Available: http://www.ingeteam.com/Portals/0/Catalogo/Sector/Documento/SSE_254_Archivo_sbp13-e01.pdf.

[42]   "Energy   recovery   systems   for   Brussels   metro".   [Online].   Available: http://www.ingeteam.com/Portals/0/Catalogo/Sector/Documento/SSE_1918_Archivo_brussels-e04.pdf.

[43] "Energy   recovery   systems   for   Malaga   C1   line".   [Online].   Available: http://www.ingeteam.com/Portals/0/Catalogo/Sector/Documento/SSE_15_Archivo_adif-malaga-energy-recovery.pdf.

[44] L. Grigans, "Rekuperētās elektriskās enerģijas izmantošana pilsētas elektrotransportā, pielietojot superkondensatorus", Rīgas Tehniskā Universitāte, 2012.

[45] P. Kreczanik, P. Venet, A. Hijazi, and G. Clerc, "Study of Supercapacitor Aging and Lifetime Estimation According to Voltage, Temperature, and RMS Current", *IEEE Trans. Ind. Electron.*, vol. 61, no. 9, pp. 4895–4902, Sep. 2014.

[46] R. Barrero, X. Tackoen, and J. Van Mierlo, "Analysis and configuration of supercapacitor based energy storage system on-board light rail vehicles", in *Power Electronics and Motion Control Conference, 2008. EPE-PEMC 2008. 13th*, 2008, pp. 1512–1517.

[47] Y. Cheng and J. Van Mierlo, "Configuration and Verification of the Supercapacitor Based Energy Storage as Peak Unit in Hybrid Electric Vehicles", in *EPE 2007Conference Proceedings*, Aalborg, p. 2007.

[48] R. Barrero, J. Van Mierlo, and X. Tackoen, "Enhanced Energy Storage Systems for Improved On-Board Light Rail Vehicle Efficiency", *IEEE Veh. Technol. Mag.*, no. 1, pp. 26–36, 2008.